Biochemical Society Transactions (2019) **47** 1041–1065
https://doi.org/10.1042/BST20180399

PORTLAND PRESS

Review Article

Visualizing the inner life of microbes: practices of multi-color single-molecule localization microscopy in microbiology

Ilijana Vojnovic, Jannik Winkelmeier and Ulrike Endesfelder

Single-Molecule Microbiology Group, Department of Systems and Synthetic Microbiology, Max Planck Institute for Terrestrial Microbiology and LOEWE Center for Synthetic Microbiology (SYNMIKRO), Marburg, Germany

Correspondence: Ulrike Endesfelder (ulrike.endesfelder@synmikro.mpi-marburg.mpg.de)

In this review, we discuss multi-color single-molecule imaging and tracking strategies for studying microbial cell biology. We first summarize and compare the methods in a detailed literature review of published studies conducted in bacteria and fungi. We then introduce a guideline on which factors and parameters should be evaluated when designing a new experiment, from fluorophore and labeling choices to imaging routines and data analysis. Finally, we give some insight into some of the recent and promising applications and developments of these techniques and discuss the outlook for this field.

Introduction

The emerging field of Single-Molecule Localization Microscopy (SMLM) allows to resolve biological structures at the nanometer scale and to monitor molecular interactions in the millisecond range. To tackle the diverse biological and technical demands of specific research questions, a growing number of practical SMLM tools have been developed over the last years. This is nicely illustrated by recent general reviews on super-resolution microscopy developments [1–3] as well as by reviews focusing on photoswitchable fluorophores needed for SMLM techniques [4–6].

However, since each research field has its own particularities, only a subset of the overall SMLM toolbox matches the given, field-specific requirements. An example of such a specific research area is the field of microbiology. Technical demands are largely shared by this field of biology, which encompasses all known microorganisms. Robust SMLM tools for studying microbial cell biology all face the challenges that microorganisms, in general, are (1) small and densely packed single-cell organisms protected by robust cell walls, (2) show rather low protein copy numbers often combined with specific autofluorescence or background of colorful pigments when compared with, e.g. mammalian cells and (3) possess rather fast growth rates accompanied by rapid metabolism rates. However, many model organisms provide widely established genetic modification tool sets facilitating genetic target labeling.

While current (microbial) SMLM studies mostly examine the dynamic and structural properties of a single target [7–9], one could argue that biological processes, in general, rely on interactions of multiple components. Therefore, establishing reliable methods for multi-color SMLM is becoming increasingly more important.

Hence, in this review, we exclusively focus on the multi-color single-molecule imaging and tracking studies on microbial cell biology published to date and discuss their utilized tools' advantages and disadvantages as well as possible pitfalls. Moreover, we highlight recent and potential future developments within the field.

Received: 2 December 2018
Revised: 22 April 2019
Accepted: 26 April 2019

Version of Record published:
11 July 2019

PORTLAND PRESS

Biochemical Society Transactions (2019) **47** 1041–1065
https://doi.org/10.1042/BST20180399

Principle of SMLM techniques

Fluorescence microscopy is a powerful tool to investigate biological systems as it allows to monitor the spatio-temporal behavior of virtually any, fluorescently labeled biomolecule of interest at high specificity. Nevertheless, even for specifically chosen, labeled molecules, details below 200 nm remain unresolved due to the diffraction barrier of light microscopy (Figure 1a, left).

Basic working principle of SMLM imaging

SMLM techniques achieve a higher resolution than conventional fluorescence microscopy methods by controlling the fluorescent emission of individual fluorophores. By a 'blinking signal' strategy, images of varying, small subsets of fluorophores can be acquired over time and the centroid of each, individual fluorescent signal can be localized at high precision to create detailed molecular maps and super-resolved SMLM images at the nanometer scale (Figure 1a, right).

Fluorophores for SMLM imaging

The most commonly used fluorophores in SMLM imaging are fluorescent proteins (FPs) and organic dyes. FPs offer the advantage of genetic labeling and consist of a β-barrel protein structure protecting the chromophore in its middle (Figure 1b, left). Organic dyes, on the other hand, usually offer higher fluorescence quantum yields than FPs and can be customized during their chemical synthesis, e.g. fine-tuning their spectral properties by a distinct delocalized π-electron system design and increasing their solubility and photostability by additional groups flanking the chromophore. Furthermore, their application is highly flexible as variable labeling groups can be added (Figure 1b, right).

Strategies in fluorophore photoswitching

Most critical in SMLM imaging is the tight control of fluorophore blinking in order to resolve individual fluorescent signals. In general, all SMLM methods can be categorized into reversible and irreversible blinking strategies (Figure 1c). For reversible blinking, two main strategies exist: fluorophores can either be imaged while reversibly binding and unbinding their targets (such as in Points Accumulation for Imaging in Nanoscale Topography (PAINT) microscopy [10]), or they can be photophysically or photochemically switched between a fluorescence-emitting and a dark state by specific light illumination and/or imaging buffers (such as in direct STochastic Optical Reconstruction Microscopy (dSTORM) [11] or by several Dark State Pumping and Recovery methods [12–16] (to which we, for simplicity, refer to by using the acronym DaStPuRe) (Figure 1c, left).

The second type of fluorophores (such as FPs used in photoactivated localization microscopy (PALM) [17]) is irreversibly photoactivated or -converted from a dark or initial fluorescent state of different color into a fluorescent state of desired read-out color (Figure 1c, right). The majority of irreversible photoactivating/converting fluorophores require UV-light illumination for changing their state. Nevertheless, recently, a novel mechanism called primed photoconversion was discovered where a special class of FPs was found to be photoconvertible via an intermediate dark state upon irradiation with less phototoxic blue and infra-red (IR) light [18,19]. Detailed reviews focusing on the photophysical and/or photochemical specifics to blink fluorophores in SMLM imaging can be found elsewhere [2,4–6].

Systematic review of multi-color SMLM studies conducted in microbes

Most studies introducing new multi-color SMLM tools are conducted in mammalian cell systems, as they contain defined and accessible nanostructures (such as cytoskeletal networks [20,21], clathrin-coated pits [22], nuclear pores [23,24] or the human glycine receptor [25]) to benchmark the tools (e.g. SMLM-suitable fluorophores such as in [2], table 2). Since a direct technology transfer to microbial targets—also from our own experience—often proves to be challenging, we compiled a systematic review of all multi-color SMLM work on microbial targets which are published to date and summarized them in Table 1 for bacteria and Table 2 for fungi. Furthermore, we assembled two visual collections of 'best-practice' examples: one for structural studies (Figure 2) and one for dynamic single-particle tracking (SPT) studies (Figure 3).

We use this systematic summary as a basis to discuss and compare the strengths, similarities and differences between current approaches and with respect to the inherent requirements for specific microorganisms. As one of the most crucial decisions when planning a new SMLM study is the choice of label and labeling technique

Biochemical Society Transactions (2019) **47** 1041–1065
https://doi.org/10.1042/BST20180399

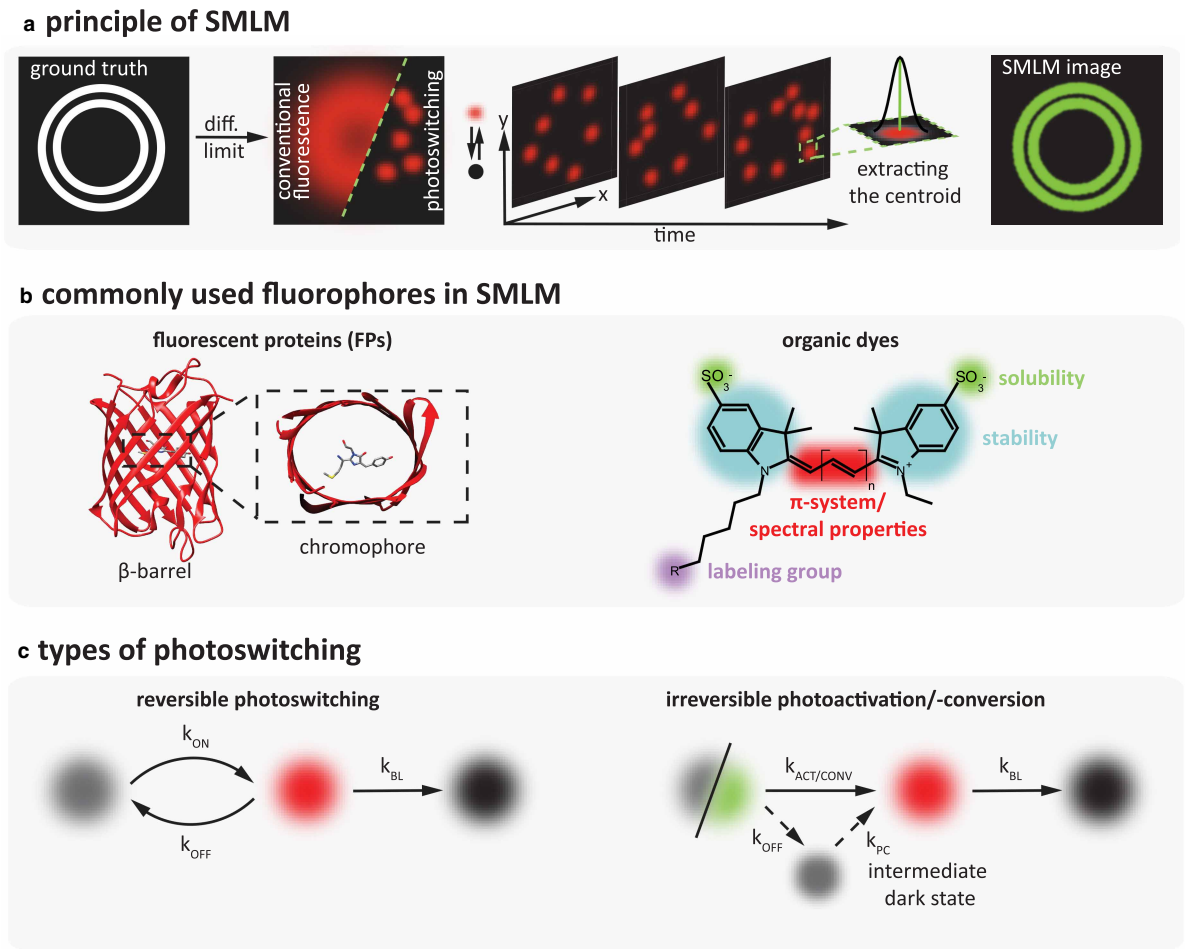

Figure 1. Principles of SMLM imaging.

(**a**) Schematic representing the basic working principle of SMLM imaging. The example ground truth of two rings is masked by diffraction in conventional fluorescence microscopy (left). The spatiotemporal separation of fluorophores by photoswitching allows to image only a subset (middle). After recording different subsets of fluorescent signals over time, their centroids are extracted and a super-resolved SMLM image can be reconstructed (right). (**b**) Commonly used fluorophores in SMLM imaging are FPs (left) and organic dyes (right). FPs consist of a β-barrel protein structure protecting a chromophore formed by three amino acid residues in its middle (left). Organic dyes are chemically synthesized to form a delocalized π-electron system (red) which, dependent on their design, can emit fluorescence at customized wavelengths (right). Additionally, the dyes are photostabilized and improved for solubility by structures flanking the chromophore. Due to variable labeling groups (violet), organic dyes can be used to specifically and flexibly label different target molecules. (**c**) Fluorophores in SMLM imaging need to possess a precisely controlled photoswitching mechanism. Some fluorophores are reversibly photoswitched between a dark state and a fluorescence emitting state (left). Here, the fluorophore either photoswitches back to the dark state or irreversibly photobleaches. Photoactivatable fluorophores irreversibly switch from a dark state to a fluorescent state by UV-light illumination, photoconvertible fluorophores switch from one fluorescent state to another (right). Certain photoconvertible fluorophores can, alternatively to the UV-light-mediated pathway, be transferred to an intermediate dark state by blue light to then subsequently convert into the fluorescent read-out state by IR light (primed photoconversion). In all cases, the fluorophores eventually photobleach.

and the available options are one of the most limiting factors in current study designs, we additionally compiled a figure introducing and explaining them for the different classes of biomolecules—proteins, carbohydrates, lipids and nucleotides—and discuss them along with our literature review below (Figure 4). The references in the caption of Figure 4b–d link the interested reader to original literature which uses those methods for targets in microorganisms.

Table 1 Multi-color SMLM studies conducted in bacteria

	Organism	Live/ fixed	Probes	Biological target	Targeting method	Technique	Imaging routine	Ref.
Triple-colored SMLM	*Caulobacter crescentus*	Live	eYFP PAmCherry NileRed	CreS PopZ Cell membrane	Chromosomal ectopic addition Dynamic on-/off-binding	DaStPuRe PALM PAINT	Parallel read-out of eYFP and PAmCherry, NileRed was added and read-out after a full read-out of PAmCherry	[14]*
	Escherichia coli	Fixed	PAmCherry NileRed, R6G AF647	RNA polymerase Cell membrane DNA	Chromosomal replacement Dynamic on-/off-binding Supplied EdU, click chemistry	PALM PAINT dSTORM	Full read-out of PAmCherry, then NileRed was added and read-out, last DNA-incorporated EdU was stained with AF647 and read-out	[26]*
			PAmCherry NileRed AF647	OmpR Cell membrane DNA	Chromosomal ectopic addition Dynamic on-/off-binding Supplied EdU, click- chemistry	PALM PAINT dSTORM	Sequential read-out, see [26] above	[27]
			mEos3.2-A69T PAmCherry NileRed SYTOX Orange	RNA polymerase FtsZ Cell membrane DNA	Chromosomal replacement Plasmid Dynamic on-/off-binding Nucleic acid-binding dye	PC-PALM PALM PAINT Diff. limited	Sequential read-out: mEos3.2-A69T, PAmCherry, subsequent addition and read-out of NileRed and SYTOX Orange	[28]*
			JF503-Hoechst NileRed AF647	DNA Cell membrane Nascent DNA	Dynamic on-/off-binding Supplied EdU, click chemistry	PAINT dSTORM	DNA-incorporated EdU was stained with AF647 and read-out, subsequent addition and read-out of NileRed and JF503-Hoechst	[29]
			PAmCherry JF503-Hoechst Potomac Red	HisB, RNAP DNA Cell membrane	Chromosomal ectopic addition Dynamic on-/off-binding	PALM PAINT	Full read-out of PAmCherry, subsequent read-out of Potomac Red and JF503-Hoechst. PAINT dyes can be applied before imaging	
Dual-colored SMLM	*Bacteroides thetaiotaomicron*	Live	TMR AF488	SusG Maltoheptose, amylopectin	Protein tag, chromosomal replacement Supplied fluorescently labeled compounds	dSTORM	Parallel read-out	[30]
		Fixed	TMR AF488	SusG SusG, -D, -E, -F	Protein tag, chromosomal replacement Immunofluorescence			
	Caulobacter crescentus	Live	eYFP PAmCherry	ParB, ParA-G16V PopZ	Plasmid	DaStPuRe PALM	Alternating read-out in two channels	[31]
			eYFP NileRed, DCDHF-Tail	CreS Cell membrane	Chromosomal ectopic addition Dynamic on-/off-binding	DaStPuRe PAINT	Read-out of eYFP, addition and read-out of membrane-binding dye	[32]
		Fixed	eYFP PAmCherry	RNase E PopZ	Plasmid	DaStPuRe PALM	Parallel read-out	[12]*
			eYFP Rhodamine Spirolactam 9	RNase E cell surface	Plasmid Dynamic on-/off-binding	DaStPuRe PAINT		
	Escherichia coli	Live	Dronpa PAmCherry	ZapA, ZapB FtsZ, ZapA	Plasmid	PALM	Parallel read-out	[33]*
			mEos3.2-A69T PAmCherry	RNA polymerase FtsZ	Chromosomal replacement Plasmid	PC-sptPALM sptPALM	Sequential read-out: mEos3.2-A69T, then PAmCherry	[28]
		Live, fixed	PAmCherry AF647	RNA polymerase DNA	Chromosomal replacement Supplied EdU, click chemistry	sptPALM dSTORM	Read-out of PAmCherry, then fixation and labeling of DNA-incorporated EdU with AF647 followed by read-out	[26]
			GFP	Fis, ParB	Chromosomal ectopic addition; FROS: chromosomal ectopic addition of parS at ori/ter	Diff. limited	Sequential read-out of first GFP then subsequent addition of both NileRed and JF646-Hoechst and imaging	[29]*
			NileRed JF646-Hoechst	Cell membrane DNA	Dynamic on-/off-binding	PAINT		

Continued

Biochemical Society Transactions (2019) **47** 1041–1065
https://doi.org/10.1042/BST20180399

Table 1 Multi-color SMLM studies conducted in bacteria

Organism	Live/ fixed	Probes	Biological target	Targeting method	Technique	Imaging routine	Ref.
	Fixed	PAmCherry NileRed	OmpR, RNA polymerase Cell membrane	Chromosomal ectopic addition (OmpR), replacement (RNAP) Dynamic on-/off-binding	PALM PAINT	Read-out of PAmCherry, then addition and imaging of NileRed	[27]
		AF647 AF568	SgrS ptsG mRNA	smFISH	dSTORM	Sequential read-out of AF647, then AF568	[34]
		ATTO655 TMR	FlgE FliO	Protein tag, chromosomal replacement	dSTORM	Parallel read-out	[35]*
		AF647, mEos3.2-N mEos3.2-C	EF-Tu MreB	Protein tag, plasmid Chromosomal replacement	dSTORM BiFC-PALM BiFC-PALM	Sequential read-out of AF647, then mEos3.2 mEos3.2-N-EF-Tu and MreB-mEos3.2-C can be used for live cell sptPALM of MreB-EF-Tu interactions	[36]
		mEos2 AF647	EF-Tu MreB	Chromosomal replacement Immunofluorescence	PALM dSTORM	Sequential read-out of AF647, then mEos2	
		AF647 AF488 Propidium iodide	FtsZ Cell surface DNA	Immunofluorescence Supplied fluorescently labeled WGA Nucleic acid-binding dye	dSTORM Diff. limited	Sequential read-out	[37]
		AF555 TOTO-3	FtsZ DNA	Immunofluorescence Nucleic acid-binding dye	dSTORM		
		JF503-/JF549-/ JF646-Hoechst Potomac Gold	DNA Cell membrane	Dynamic on-/off-binding	PAINT	Sequential addition and read-out of PAINT dyes	[29]
Salmonella typhimurium	Live	ATTO655 TMR-Star	CheZ CheY	Protein tag, plasmid	dSTORM	parallel read-out	[38]
	Fixed	TMR ATTO655	FliM FliC	Protein tag, chromosomal replacement Immunofluorescence	dSTORM	Sequential read-out of TMR and ATTO655, parallel read-out of TMR-Star and ATTO655/SiR	[39]
		ATTO655 TMR-Star	SpaS, FliN FliN, SpaS	Protein tag, chromosomal replacement			
		SiR TMR-Star	SiiF SiiC	Protein tag, plasmid			
		mEos3.2 AF647	PrgH, SpaO SipD	Chromosomal replacement immunofluorescence	PALM dSTORM	Sequential read-out of AF647, then mEos3.2	[40]*
Vibrio cholerae	Live	AF405-Cy5 Cy3-Cy5 DAPI	RbmC Vibrio polysaccharide DNA	Protein tag, chromosomal replacement Supplied fluorescently labeled WGA Nucleic acid-binding dye	STORM Diff. limited	Alternating activation of acceptor dyes (AF405 or Cy3) with a continuous read-out of receptor dye Cy5, then DAPI read-out	[41]*

Continued

Biochemical Society Transactions (2019) **47** 1041–1065
https://doi.org/10.1042/BST20180399

PORTLAND PRESS

Table 1 Multi-color SMLM studies conducted in bacteria

Part 3 of 3

	Organism	Live/ fixed	Probes	Biological target	Targeting method	Technique	Imaging routine	Ref.
Single-colored SMLM + 1 diff. limited color	*Bacillus subtilis*	Live	SytoxGreen FM4-64 mMaple	DNA cell membrane SpoIIIE	Nucleic acid-binding dye Membrane-binding dye Chromosomal ectopic addition in ΔSpoIIIE strain	Diff. limited PALM	Sequential read-out of SytoxGreen, then Maple, last addition and read-out of FM4-64	[42]
			PAmCherry mCitrine	MutS DnaX	chromosomal replacement (MutS), ectopic addition (DnaX)	sptPALM Diff. limited	Sequential read-out of mCitrine and then PAmCherry	[43]*
			FM5-95 Dendra2, tdEos	cell membrane SpoIIIE	membrane-binding dye chromosomal replacement	Diff. limited PALM	Sequential read-out of FM5-95, then Dendra2 or tdEos	[44,45]
	Caulobacter crescentus	Live, fixed	eYFP CFP, mCherry	ParA ParB	Chromosomal ectopic addition	DaStPuRe Diff. limited	Read-out of mCherry/CFP spot, followed by a high laser illumination forcing most eYFP molecules into a dark state allowing to read-out single spots	[16]
	Escherichia coli	Live	eYFP mEos2	hdeA, hchA, lacZ genes H-NS	FROS: chromosomal ectopic addition of TetR-eYFP and TetO array next to targets Chromosomal replacement	Diff. limited PALM	Sequential read-out of mEos2 and eYFP	[46]
			PAmCherry Syto-16	UvrA, UvrB DNA	Chromosomal replacement Nucleic acid-binding dye	sptPALM Diff. limited	Sequential read-out of Syto-16, then PAmCherry	[47]*
			PAmCherry SytoxGreen	RNA polymerase DNA	chromosomal replacement Nucleic acid-binding dye	PALM Diff. limited	Sequential read-out of SytoxGreen, then PAmCherry	[48]
			PAmCherry GFP	lacO array malO array	FROS: chromosomal ectopic addition of 6× tandem lacO and lacI-PAmCherry FROS: chromosomal ectopic addition of 20× malO next to lacO array, MalI-GFP: plasmid	PALM Diff. limited	Sequential read-out of PAmCherry, then GFP	[49]*
		Fixed	AF647 YOYO-1	FtsZ DNA	Immunofluorescence Nucleic acid-binding dye	dSTORM Diff. limited	Sequential read-out of YOYO-1, then AF647	[50,51]
			mKate2 YPet	UmuC LacY	Chromosomal replacement Plasmid	Diff. limited DaStPuRe	Sequential read-out of mKate2, followed by a high laser illumination forcing most eYFP molecules into a dark state allowing to read-out single spots	[52]

The table is structured as follows (left to right): (1) number of (SMLM) colors used, (2) investigated microorganism in alphabetical order, (3) live, live/fixed or fixed study, (4) applied fluorophore combination sorted by sequential read-out order or excitation wavelength for parallel read-out, (5) biological targets, (6) targeting method; ectopic addition: an additional copy of the POI gene with tag sequence is introduced into the organism by chromosomal integration at another locus, replacement: fusion replaces the POI gene at original locus under the original promoter, (7) SMLM method; DaStPuRe: dark state pumping and recovery, illumination with high laser power forces the fluorophores into a dark state, (8) comments to imaging procedure, (9) references (* highlights studies that are represented in Figures 2 and 3).

Biochemical Society Transactions (2019) **47** 1041–1065
https://doi.org/10.1042/BST20180399

Table 2 Multi-color SMLM studies conducted in fungi

Part 1 of 2

	Organism	Live/ fixed	Probes	Biological target	Targeting method	Technique	Imaging routine	Ref.
Dual-colored SMLM	*Saccharomyces cerevisiae*	Live	mKate2 YPet	Pil1 Sur7, Lyp1, Can1	Chromosomal replacement	DaStPuRe	A high laser illumination forces most mKate2 molecules into a dark state which allows to read-out single spots, then same procedure for YPet	[13]*
			mCardinal	Can1, Nha1, Pma1	Chromosomal replacement (Can1), plasmid (Can1, Nha1, Pma1)	SPT	First SPT using mCardinal, then YPet read-out as above	
			YPet	Sur7	Chromosomal replacement	DaStPuRe		
		Fixed	AF647 AF700	Cdc11 α-linked mannose	Chromosomal replacement (GFP fusion), immunofluorescence (anti-GFP nanobody) Fluorescently labeled concanavalin A	dSTORM	Parallel spectral demixing read-out	[53]*
			AF647 tdEos	α-linked mannose α-tubulin	Fluorescently labeled concanavalin A Chromosomal replacement (one of two α-tubulin genes of diploid)	dSTORM PALM	Sequential (AF647 then tdEos) on a multifocus microscope	[54]*
			AF647 AF750	Tub4 Tub1	mCherry (γ-tubulin) and GFP (α-tubulin) fusions, immunofluorescence (anti-GFP/ RFP nanobodies)	dSTORM	Parallel spectral demixing read-out	[55]
			AF647 mMaple	Las17, Myo5 Sla2, Abp1, Las17	Protein tag, chromosomal replacement Chromosomal replacement	dSTORM PALM	Parallel read-out	[56]*
			AF647 mMaple	Sla2 Ede1	Chromosomal replacement (GFP fusion), immunofluorescence (anti-GFP nanobody) Chromosomal replacement	dSTORM PALM		

Continued

Biochemical Society Transactions (2019) **47** 1041–1065
https://doi.org/10.1042/BST20180399

PORTLAND PRESS

Table 2 Multi-color SMLM studies conducted in fungi Part 2 of 2

	Organism	Live/ fixed	Probes	Biological target	Targeting method	Technique	Imaging routine	Ref.
	Schizosaccharomyces pombe	Live, fixed	Dendra2 PAmCherry DAPI	cbp1 cnp1 DNA	Chromosomal replacement Nucleic acid-binding dye	PC-sptPALM sptPALM Diff. limited	Sequential read-out of Dendra2, PAmCherry, then fixation, addition and read-out of DAPI	[28]*
		Fixed	mMaple3	19 structural, 10 signaling contractile ring POIs, lifeact, Acyl	Chromosomal replacements (contractile ring proteins), plasmid (Acyl, lifeact)	PALM	Sequential read-out of Atto647N and either AF488 (for both dyes, PALM-like read-out with 405 nm activation without imaging buffer was used) or one of the mMaple3 tagged ring components.	[15]
			ATTO647N	Cell membrane	Fluorescently labeled mCling	DaStPuRe		
			AF488 ATTO647N	Actin Cell membrane	Fluorescently labeled phalloidin Fluorescently labeled mCling	DaStPuRe		
			mScarlet-I mEos3.2-A69T PAmCherry	sad1 spc25 cnp1	Chromosomal replacement	Diff. limited PC-PALM PALM	Full read-out of mScarlet-I, mEos3.2-A69T, then PAmCherry	Unpub#*
Single-colored SMLM + 1 diff. limited color	*Saccharomyces cerevisiae*	Fixed	mEos2	PI3P	Plasmid ($[FYVE]_2$ domain of EEA1 targeting PI3P)	PALM	Sequential read-out of mEos2, then GFP	[57]
			GFP	Chc1, Clc1, Vps21, Ypt7	Plasmid	Diff. limited		
			mMaple	Las17, Ede1, Pam1, Abp1	Chromosomal replacement	PALM	Sequential read-out of mMaple, then GFP	[56]
			GFP	Abp1, Sla2, Rvs167	Chromosomal replacement	Diff. limited		
	Ustilago maydis	Live	tdEosFP GFP	Num1 Tub1	Chromosomal replacement Chromosomal ectopic addition	PALM Diff. limited	Sequential read-out of GFP, then tdEosFP	[58]
		Fixed	tdEosFP GFP	Num1 Rab5a	Chromosomal replacement Chromosomal ectopic addition	PALM Diff. limited		
	Aspergillus nidulans	Live	mEosFPthermo GFP	TeaR tubA, SecC	Chromosomal ectopic addition	PALM Diff. limited	Parallel read-out	[59]

See the explanation of Table 1, #unpublished work from our group [60]. *highlights studies that are represented in Figures 2 and 3.

Biochemical Society Transactions (2019) **47** 1041–1065
https://doi.org/10.1042/BST20180399

Biochemical Society Transactions (2019) **47** 1041–1065
https://doi.org/10.1042/BST20180399

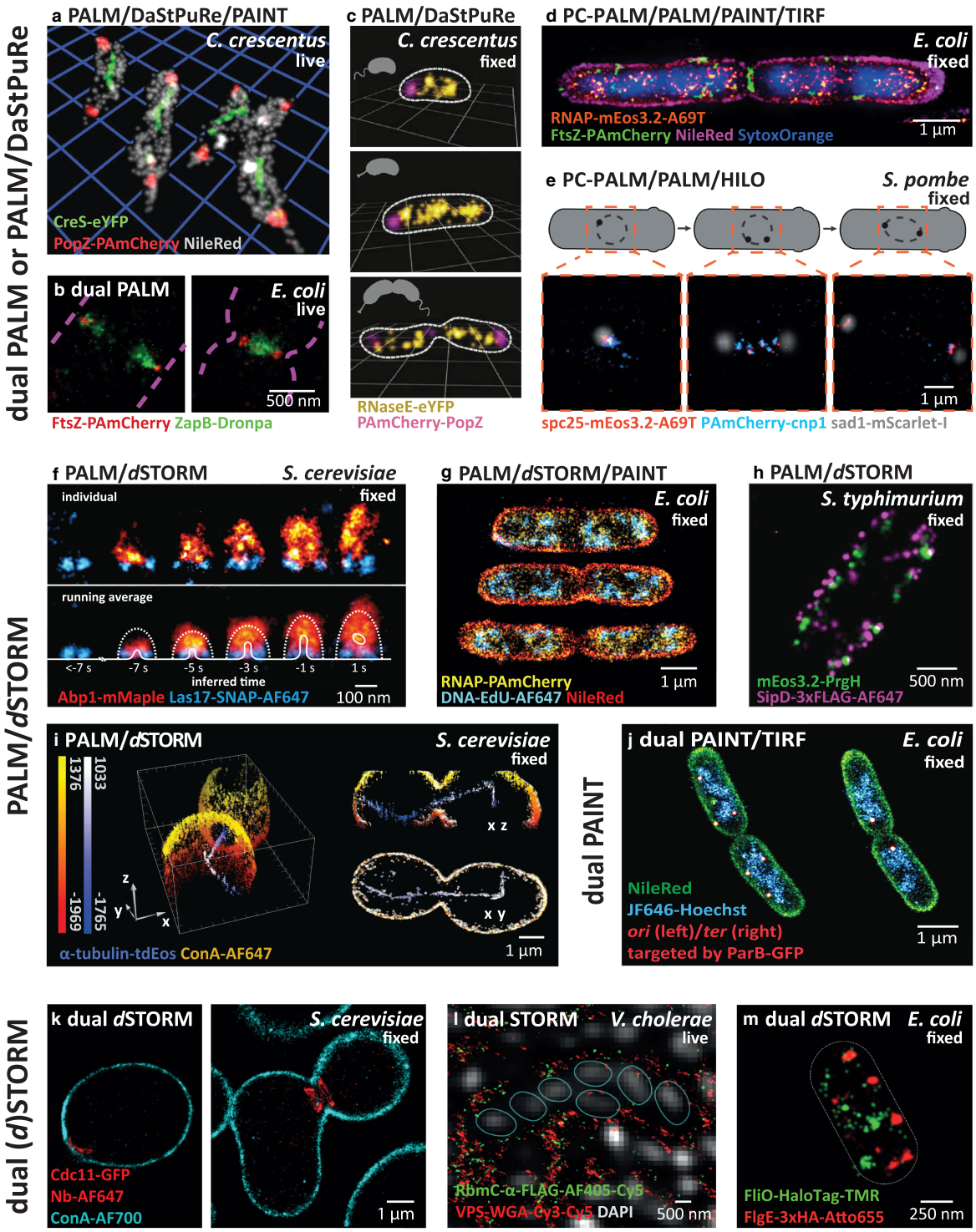

Figure 2. Examples of structural multi-color SMLM studies in microorganisms. Part 1 of 2

(**a**) Co-localization of filament-like fiber and pole-organizing protein structures in live *Caulobacter crescentus*. Grid segments: 1 µm adapted with permission from [14]. Copyright 2013 American Chemical Society, (**b**) Divisome elements during different cell cycle stages in live *E. coli* cells. Adapted from [33]. Copyright CC BY 4.0, (**c**) RNA degradosome and pole-organizing protein structures in fixed *C. crescentus* cells undergoing different cell cycle stages. Grid segments: 1 µm. Adapted from [12]. Copyright CC BY 4.0, (**d**) Co-localization of a transcriptome machinery compartment, a divisome element and the nucleoid in fixed *E. coli*. [28]. Copyright CC BY 4.0, (**e**) Spindle pole and kinetochore components during different cell cycle stages in

Biochemical Society Transactions (2019) **47** 1041–1065
https://doi.org/10.1042/BST20180399

Figure 2. Examples of structural multi-color SMLM studies in microorganisms. Part 2 of 2

fixed *Schizosaccharomyces pombe* (Unpublished work, [60]), (**f**) Endocytosis machinery compartments in fixed *S. cerevisiae* cells. Adapted from [56]. Copyright CC BY 4.0, (**g**) Transcriptome co-localized with nucleoid structure in fixed *E. coli*. © IOP Publishing. Adapted with permission from [26]. All rights reserved. (**h**) Type III protein secretion machinery compartments in fixed *Salmonella typhimurium*. Adapted from [40]. Copyright CC BY 4.0. (**i**) Yeast microtubules during cell division in fixed *S. cerevisiae*. Adapted from [54]. Copyright CC BY 4.0. (**j**) Nucleoid structure in fixed *E. coli* cells. Adapted from [29]. Copyright CC BY 4.0. (**k**) Septin ring component co-localized with the membrane in fixed *S. cerevisiae*. Adopted by permission from [53], (**l**) Extracellular polysaccharide and protein distributions in live *Vibrio cholerae* biofilms. Adapted from [41] with permission from AAAS. (**m**) Flagellar-specific type III secretion system components in fixed *E. coli*. Adapted from [35]. Copyright CC BY 4.0.

Multi-color microbial SMLM studies are still rare

At a first glance, our compilation demonstrates that multi-color SMLM work is still exceptional in microbiology as we count only 40 studies (Tables 1 and 2). Most multi-color studies either investigate only one target at high resolution accompanied by a diffraction-limited structural reference such as the nucleoid, cell membrane or a single-spot-forming protein cluster (15 studies, examples are Figure 3a–c[43,47,49]) or two targets at high resolution (20 studies, examples are Figures 2b,c,f,h–k,m and 3d,f [12,13,26,29,33,35,40,53,54,56]) also often supported by a reference (Figures 2e,l and 3e [28,41,60]). Three targets in SMLM resolution are rare (five studies, examples are Figure 2a,d,g [14,26,28]), and studies aiming at four or more targets are non-existent (to our knowledge).

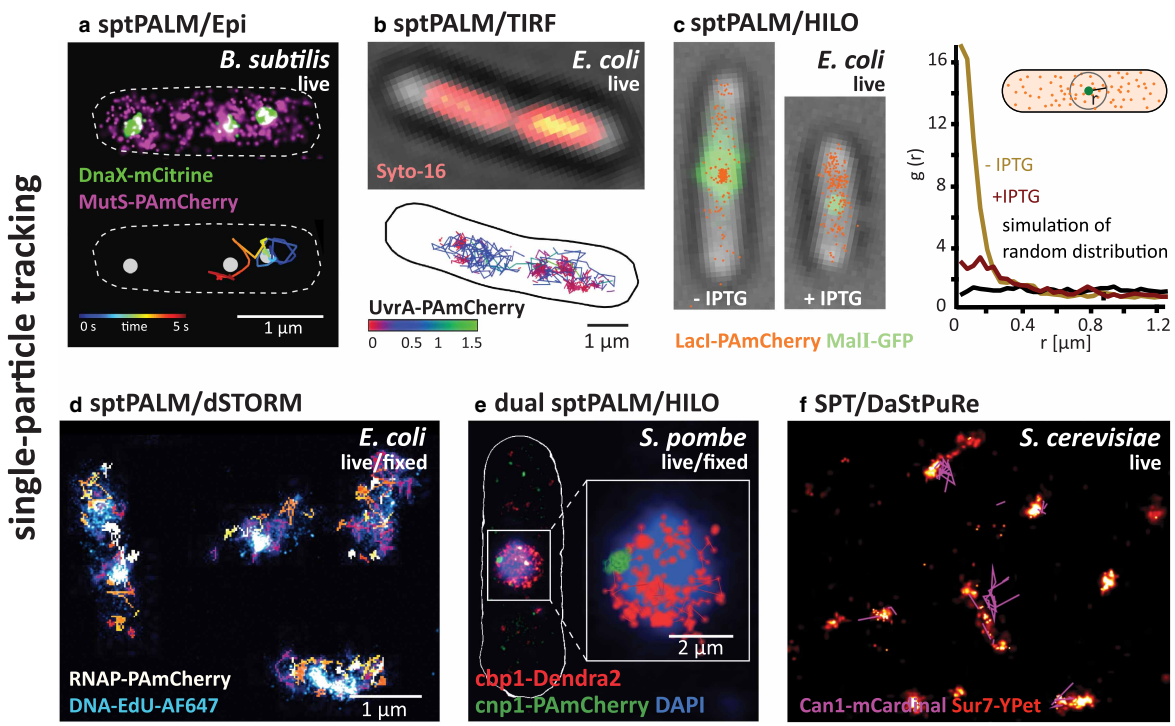

Figure 3. Examples of multi-color SPT studies in microorganisms.

(**a**) Co-localization of a DNA repair component and a DNA replication gene in live *B. subtilis*. Adapted from [43]. Copyright CC BY 4.0. (**b**) Nucleotide excision repair components in live *E. coli*. Adapted from [47]. Copyright CC BY 4.0. (**c**) Transcription factor distributions at specific gene locations in live *E. coli*. Adapted from [49]. Copyright CC BY 4.0., (**d**) Transcriptome co-localized with nucleoid structure in live *E. coli*. © IOP Publishing. Adapted with permission from [26]. All rights reserved. (**e**) Co-localization of centromeres and kinetochore-associated DNA binding proteins. Adapted from [28]. Copyright CC BY 4.0. (**f**) Membrane compartments and proteins in live *S. cerevisiae*. Adapted from [13]. Copyright CC BY 4.0.

Biochemical Society Transactions (2019) **47** 1041–1065
https://doi.org/10.1042/BST20180399

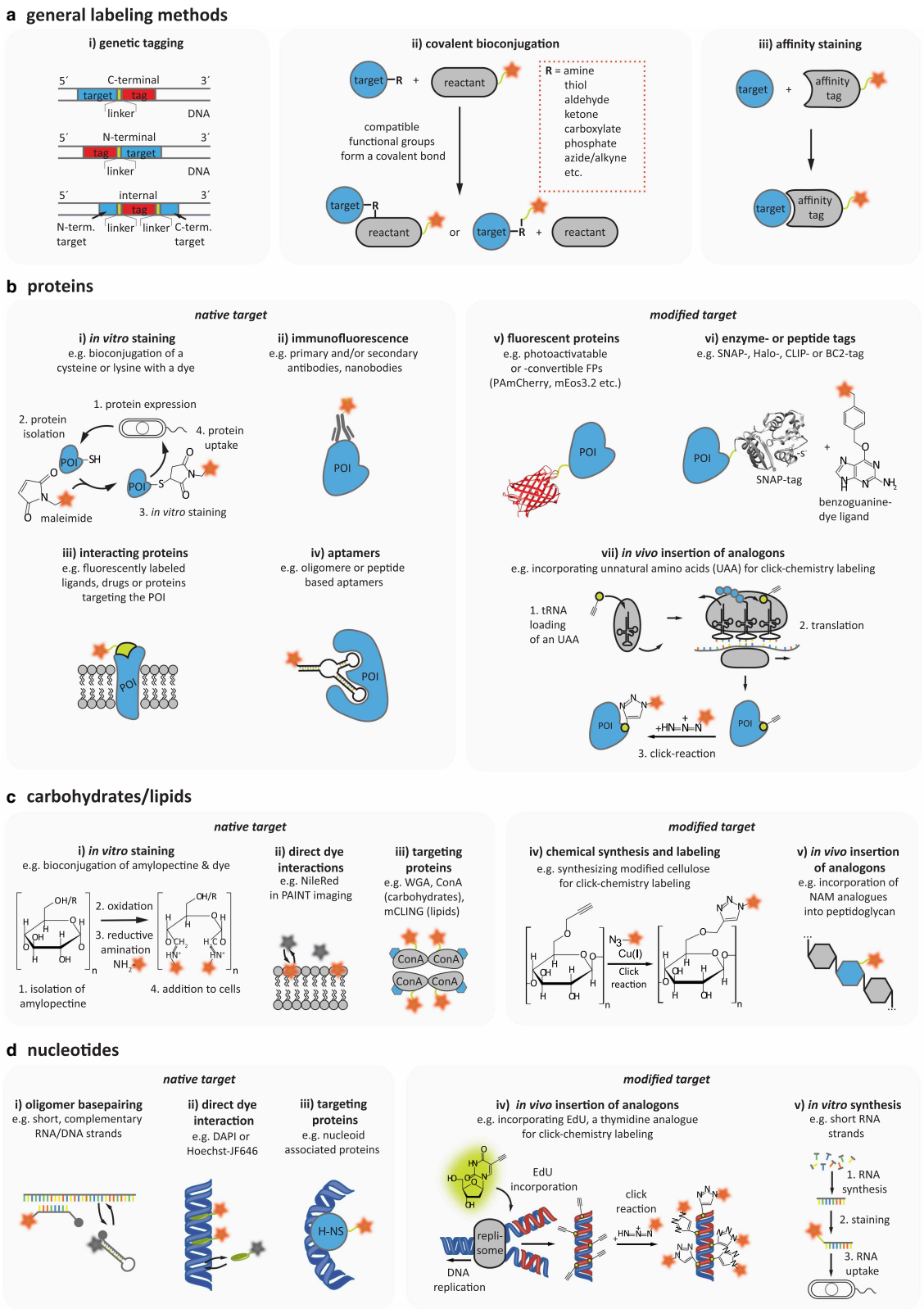

Figure 4. SMLM-suitable labeling methods targeting proteins, carbohydrates, lipids and nucleotides. Part 1 of 2

(**a**) Target molecules can be genetically modified (i) or stained by covalent bioconjugation (ii) or by affinity staining (iii). For genetic labeling, the chosen gene (blue) is extended by a tag sequence, e.g. encoding for an FP, enzyme- or peptide tag (red).

Biochemical Society Transactions (2019) **47** 1041–1065
https://doi.org/10.1042/BST20180399

Figure 4. SMLM-suitable labeling methods targeting proteins, carbohydrates, lipids and nucleotides. Part 2 of 2

It can be inserted at the 3′- or 5′-end or directly into the target sequence, e.g. replacing or extending an internal loop structure. In each case, a small linker sequence (green) is inserted in between to ensure the undisturbed biological function of the target protein (i). For labeling a molecule by covalent bioconjugation, a functional group (e.g. amines, thiols, etc.) of the target is exploited for forming a covalent bond with a fluorescently labeled reactant (ii). Molecules can also be targeted using fluorescently labeled affinity tags which bind them by van der Waals bonds or ionic attractions (iii). (**b**) Native POIs (blue) are either stained *in vitro* after their expression and isolation before being taken up again into cells [61,62] or *in situ* by adding a fluorescently labeled interacting compound, e.g. by immunofluorescence using anti- or nanobodies [36,37,39,40,50,51,53,56] (ii), by fluorescently labeled ligands, drug molecules or targeting proteins [15] (iii) or by aptamers (iv). Furthermore, the POI can be modified, either by a FP (v, PAmCherry (pdb 3KCT)) [13,14,28,40,43,58,59] or by an enzyme/peptide tag (vi, SNAP (pdb 3L00)) [21,30,35,36,38,39,41,56,63] or by insertion of an unnatural amino acid into the primary structure of the protein (vii), which after protein folding is coupled to a dye by a click chemistry reaction [64,65]. (**c**) Staining of native carbohydrates or lipids can be facilitated in a similar fashion as for proteins. In vitro staining is showcased using isolated amylopectin [30] (i). Furthermore, specific lipophilic, fluorogenic dyes can directly visualize the native membrane by reversible on- and off-binding in PAINT microscopy (ii) [14,26,28,29,42]. Also carbohydrates-targeting proteins like WGA and ConA or lipid-targeting probes like mCLING or FYVE can be used (iii) [15,37,41,53,54,57]. Synthetic carbohydrates or lipids can be customized *in vitro* (iv). Finally, also analogues of native building blocks can be inserted into newly synthesizing polymers *in vivo* (v) [66]. (**d**) Specific nucleotide sequences are labeled by single-molecule fluorescence *in situ* hybridization (smFISH) using short, complementary DNA/RNA oligomers (often designed as fluorogenic hairpins in a fluorophore–quencher combination) (i) [34]. DNA, in general, can be either visualized by the reversible on- and off-binding of fluorogenic DNA intercalator-dye constructs using DNA-PAINT (ii) [29] or by nuclear-associated proteins decorating it (iii) [46]. A method to label nascent DNA is by incorporation of the alkyne-modified thymidine analog EdU during DNA replication combined with subsequent click labeling (v) [26,27,29]. Short oligomers can also be synthesized and stained *in vitro* to then be transferred into cells, e.g. by electroporation [67,68].

Most studies investigate microbial model organisms

The vast majority was conducted in bacteria (30 studies with 18 studies at least dual color and 12 studies single-color SMLM imaging plus a diffraction-limited reference, Table 1), with the model organism *Escherichia coli* having the biggest share (13 studies). In contrast, only 12 studies focused on fungi biology (eight at least dual color, four are single-color plus reference, Table 2), among which the studies on *Saccharomyces cerevisiae* dominated by number (seven studies).

In general, for both fungi and bacteria, the great majority of studies is conducted in model organisms where laboratory cultivation techniques are well established and for which a large number of tools, e.g. genetic manipulation strategies have been developed. Multi-color SMLM studies under more complex culturing conditions (e.g. under medical relevant conditions or using non-model strains and exploring, e.g. biofilms or co-cultures like the human microbiome) are scarce (Figure 2l) [30,41].

Structural multi-color SMLM studies are established whereas SPT studies are rare

Furthermore, the studies are largely focusing on structural SMLM imaging exploring spatial molecular organizations (126 targets in total), mostly conducted in chemically fixed cells (102 fixed versus 24 live targets, Figure 2 and Tables 1 and 2). Multi-color SPT studies are rare (eight targets in total, Figure 3 and Tables 1 and 2). These SPT studies investigating molecular interactions were mostly conducted using single-color sptPALM accompanied by a diffraction-limited reference [43,47] and in one case super-resolving the nucleosome via dSTORM [26]. Investigating the dynamics of two targets was conducted by either orthogonal photoactivation modes in a subsequent manner [28] or bimolecular fluorescence complementation-PALM (BiFC-PALM), where two biological targets were each labeled with one component of a split FP [36].

Most studies record the different targets sequentially in time

Reviewing the imaging routines, fluorophore combinations were either imaged in parallel by splitting the signals of appropriate fluorophore pairs onto two areas of the camera chip (14 studies), or more commonly in a sequential imaging mode using the same detection path (28 studies). For the latter, also fluorophores of similar emission spectra can be used when separating them either by different photoactivation/conversion modes [28] or by sequential addition or exchange of probes (e.g. sequentially added dyes for PAINT imaging

[26–28] or 5-ethynyl-2′-deoxyuridine (EdU) staining of DNA [26,27]. For both methods, this brings the advantage of avoiding chromatic aberrations. When adding fluorophores sequentially, a position-stabilizing autofocus system or a robust position-refinding routine (by, e.g., re-recognizing unique landmarks) is required.

Among the diverse labeling options, genetic labeling, in particular, FP fusions, are dominant

A successful experimental multi-color design needs a thought-out choice of fluorophore combinations and labeling methods. Well-established genetic tools (Figure 4a(i)), which include powerful methods like exploiting the microbes' own homologous repair mechanism for chromosomal recombinant replacements of native target genes, exist for most model microorganisms [69]. Also, while being densely packed into the small microbial volume, absolute copy numbers of microbial protein of interests (POIs) can be rather low [70] which demands for highly specific labeling approaches. Performing statistics on all published studies summarized in Tables 1 and 2, it is thus not surprising that chromosomal tags were used for 90 out of 154 targets, 72 of which as recombinant replacements at the original locus under the original promoter and 15 as ectopic additional copies, integrated into the chromosome at another locus. These are FP fusions to a large extent (77 POIs, Figure 4b(v)) with only a minor portion of protein tags (10 chromosomal replacements, Figure 4b(vi)) and fluorescent repressor–operator system (FROS) arrays (4 ectopic additions). Additional 22 genetic fusions were introduced into the cells by plasmids carrying recombinant genes. Other targeting methods are only seldom applied: We find 14 immunofluorescence stainings (10 antibody stainings targeting native epitopes and 4 anti-GFP/-RFP nanobody probes, Figure 4a(iii) and b(ii)), 17 uses of on- and off-binding PAINT probes (Figure 4c(ii) and d(ii)), and 12 incubations with target-specific and fluorescently labeled compounds (Figure 4a(ii), b(ii–iv), c(i–iii), d(i–iii)). For the latter, various labeling methods were used, such as (1) *in vitro*-labeled compounds (e.g. *in vitro*-labeled carbohydrates specific for the cell wall (Figure 4c(i)) [30], target-specific drugs like WGA [37,41] and concanavalin A (Figure 4c(iii)) [53,54], actin-binding phalloidin or lifeact (Figure 4b(iii)) [15] or smFISH oligonucleotides (Figure 4d(i)) [34]), (2) target-binding fluorophores (e.g. TOTO-3 targeting DNA (Figure 4d(ii)) [37]), and (3) analogs carrying, e.g. alkene or azide groups that can be stained by click chemistry approaches afterwards (Figure 4b(ii,v), c(iv), d(iv)). For the latter, the most often used one is the thymidine analog EdU incorporating into nascent DNA (Figure 4d(iv)) [26,27,29]).

Either the DsRed-derived FP PAmCherry or an FP from the Kaede family are part of almost every multi-color labeling strategy

Turning the perspective to the selected molecules of interest, FPs strongly dominate the chosen combinations when imaging protein targets. Here, PAmCherry fulfills a special role: it is the only commonly applied photoactivatable FP of the DsRed family [5]. These photoactivatable FPs photoactivate from an initial dark, premature chromophore state into their fluorescent state in the 'red' part of the visible spectrum (~580–660 nm wavelength range). In a multi-color experiment, PAmCherry thus stands out from the RFPs from the Kaede family (e.g. mEos2 or 3, Dendra2 or mMaple(3)) as these green-to-red photoconverting FPs fluoresce in the 'green' part of the visible spectrum (~490–560 nm wavelength range) in their initial GFP-like form [5]. This makes PAmCherry an almost obligatory choice for (1) green/red dual FP pairings (being either paired with eYFP (Figure 2a,c) [12,14,31] or Dronpa (Figure 2b) [33]) and for (2) dual red FP pairings which are separated by orthogonal illumination modes when photoactivating PAmCherry by UV-light and photoconverting a FP from the Kaede family by primed photoconversion (only possible for threonine 69 variants [18], e.g. using mEos3.2-A69T (Figure 2d,e) [28,60], or Dendra2 (Figure 3e) [28]).

Another commonly used combination is far-red (~650–730 nm wavelength range) dyes together with red FPs (10 studies). Here both PAmCherry and the Kaede-like proteins are equally popular choices as the green spectral channel can be neglected (Figures 2f,g,h,i and 3d). The choice of the far-red dye is dominated by AF647—also incredibly popular in single-color dSTORM experiments (see [2], table 2)—and leads to a remarkable count of 9 out of 10 studies (examples in Figures 2f,g,h,i,k and 3d).

Target biomolecules other than proteins are mainly imaged by dSTORM and PAINT techniques

Cellular components other than proteins are usually reliant on non-genetic targeting tools and thus are mostly investigated by dSTORM and PAINT studies. In case of dual dSTORM experiments relying on organic

Biochemical Society Transactions (2019) **47** 1041–1065
https://doi.org/10.1042/BST20180399

dyes, it becomes apparent that the membrane-permeable, spectrally distinct red/far-red dye combination TMR (-Star)/ATTO655 (Figure 2m, four out of six red/far-red pairings [35,38,39]) were preferred over AF647 paired with spectrally close dyes in a spectral demixing imaging mode (AF700 (Figure 2k) [53] or AF750 [55]) or green/red [30], green/far-red [15,37] or STORM activator/acceptor (Figure 2l) [41] dye combinations.

SMLM visualization of the cell membrane was mainly conducted by using the dynamic on- and off-binding of NileRed for PAINT imaging (8 out of 17 studies of the cell membrane, Figures 2a,d,j,g and 4c(ii)[14,26–29,32]), while labeling of DNA was performed using either (a) transiently binding dyes (e.g. JF646-/JF549- or JF503-Hoechst (Figures 2j and 4d(ii)) [29], (b) EdU stainings with AF647 (Figures 2g, 3d and 4d(iv)) [26,27], (c) blinking intercalator TOTO-3 (Figure 4d(ii)) [37]) or (d) diffraction-limited fluorescent probes (DAPI (Figures 2l and 3e) [28,41], Sytox Green [42,48] or Orange (Figure 2d) [28], Syto-16 (Figure 3b) [47] or propidium iodide [37]). The most popular diffraction-limited reference is DNA (nine times), while the co-imaged SMLM probe in most cases was a red FP (seven times, out of which four times PAmCherry was chosen [28,47,48]). One study combined membrane and DNA probes for dual-PAINT, accompanied by either a FROS array spot or a PAmCherry-labeled POI (Figure 2j) [29].

For the few triple-color studies, until now dual-FP/PAINT (Figure 2a,d) [14,28], dual-PAINT/PALM [29] or PALM/PAINT/dSTORM (Figure 2g) [26,27] approaches were established.

Design of a multi-color SMLM experiment investigating microbial cell biology

Based on our observations while comparing the 40 publications applying multi-color SMLM studies in microbiology, we compiled a best practice guideline (Figure 5a and Table 3). Whereas the rationale behind this guideline can be generally used to design multi-color SMLM experiments for any organism, our examples are focused on studying microbes. Importantly, single-molecule imaging and tracking methods can yield a manifold of detailed answers about individual molecules and their interactions at a high spatiotemporal resolution *in situ*, but they are not every-samples techniques. Experimental factors such as single-molecule sensitivity beyond (low) background, tight photoswitching control of fluorophores or reliable corrections for drift and chromatic aberrations are strong determinants for image quality. Achieving good results for several channels in multi-color imaging is multiplying the overall efforts to be undertaken. To further illustrate our general scheme, we thus as well added a practical example of study design based on our own experience (Figure 5b).

Formulating the biological question

First of all, it is worthwhile to invest a lot of resources into the study's design and to precisely formulate and specify the biological question one aims to answer. This entails a profound knowledge of the underlying biological system and often goes in hand with a strong hypothesis about observations to be expected (Figure 5a, upper box). It should be clear whether the observation of a structure and/or the dynamics of how many targeted molecules leads to a relevant investigation and which spatiotemporal resolution is required to acquire the data aimed for (Figure 5a, TASK 1 and 2).

Here, a higher temporal resolution or measuring the axial position often goes hand in hand with the trade-off of a lowered lateral spatial resolution due to lowered signal-to-noise (S/N) ratio of individual single-molecule fluorescence [1]. Often, one can already 'guestimate' from the target characteristics and its cellular environment where some technical hurdles might appear, e.g. thick cell walls might hinder staining, low pH, e.g. in the periplasm, lowers fluorescence read-out or colorful microbial pigments (e.g. carotenoids, melanins or flavins [73]) can superpose fluorescence in certain spectral ranges. In cases where both target protein termini are functional domains (as often encountered for membrane receptors), genetic tagging of either of them will most likely interfere with the proteins' biology. In such cases, internal loop structures could be a better-suited spot for recombinant fusions, as has been done for, e.g., MreB in *E. coli* [74–76].

Furthermore, reflecting target abundances, their replenishment and accessibility can be of large importance: Is a native expression from the native gene locus possible and favorable (e.g. for measuring stoichiometry and cellular organization) or is an ectopic expression better suited for the planned investigation (e.g. exploring the DNA binding affinities of proteins in large statistics facilitated by overexpression and irrespective of their native copy number)? Is the time of POI folding or POI lifetime known? Too fast protein turn-over can prevent the use of FPs due to their typically rather long maturation time needed to properly arrange their chromophore and thus their ability to fluoresce [77,78]. In case of low molecular abundances or co-localization studies of

Biochemical Society Transactions (2019) **47** 1041–1065
https://doi.org/10.1042/BST20180399

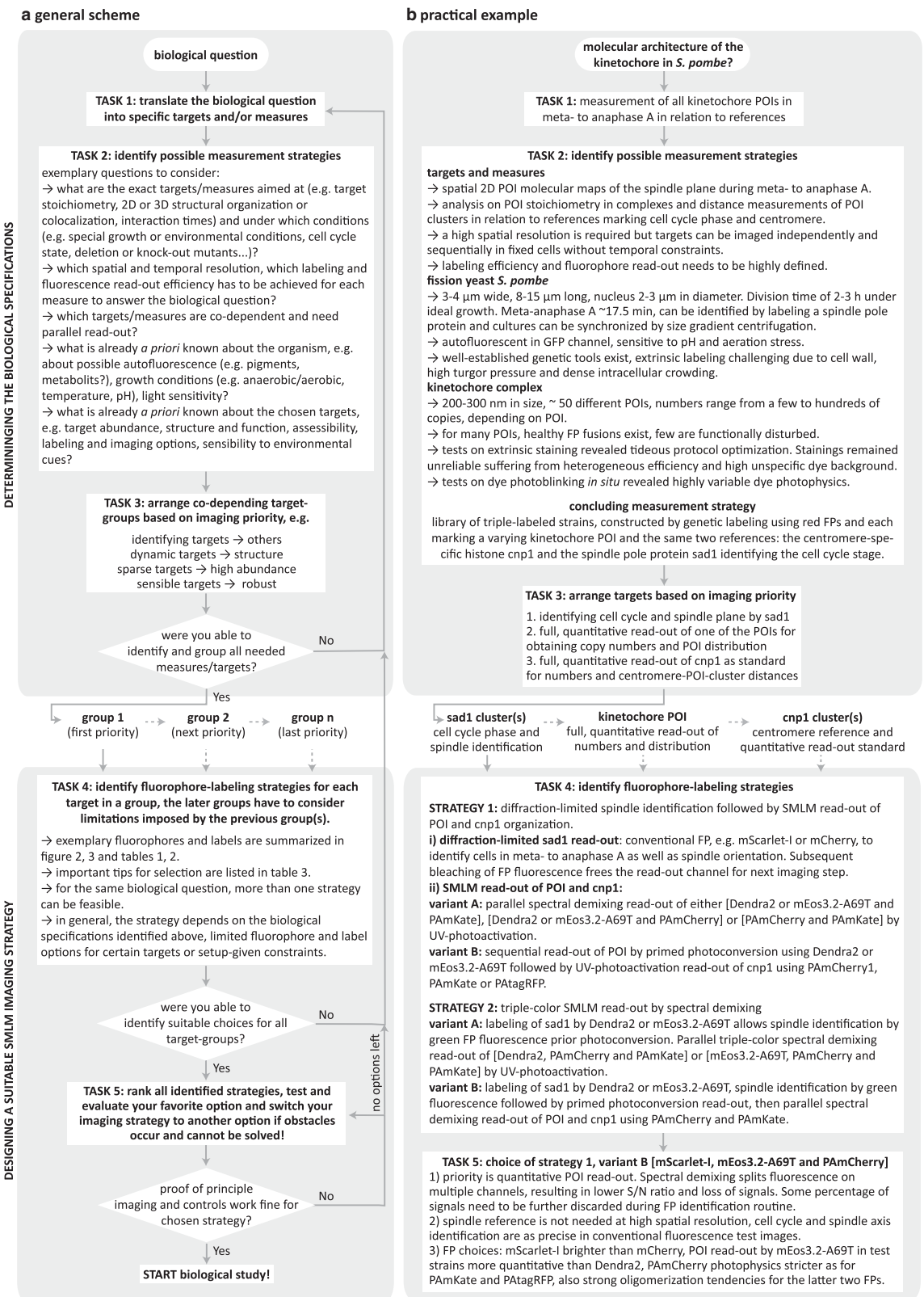

Figure 5. Guideline for designing a multi-color SMLM experiment. Part 1 of 2

(**a**) General scheme. For a successful study design, first, the biological specifications have to be determined (upper box). For this, the general biological research question needs to be translated into specific targets and measures (TASK 1). By answering

Biochemical Society Transactions (2019) **47** 1041–1065
https://doi.org/10.1042/BST20180399

Figure 5. Guideline for designing a multi-color SMLM experiment. Part 2 of 2

several target- and organism/system-related questions (TASK 2), possible measurement strategies can be identified (TASK 2) and the targets can be arranged into groups based on their imaging priority (TASK 3). If no solution can be found, the choice of measures and/or targets should be reassessed by repeating TASK 1. After a successful target grouping, the technical study design can be approached (lower box). First, a suitable fluorophore–label combination should be chosen for each target in the group, taking limitations set by groups with higher priority or setup limitations into account (TASK 4). If multiple strategies seem possible, they can be ranked based on their applicability and can be readjusted if initial test experiments show major obstacles. If none of the options yields a suitable experimental strategy, the choice of measures and/or targets has to be reassessed by repeating TASK 1. After a successful proof of principle experiment, the biological study can be started. (**b**) Practical example. To illustrate the general scheme, we added an example based on our own experience. Here, our interest in investigating the kinetochore architecture of the fission yeast *S. pombe*, a multi-protein complex linking microtubules and centromeric DNA during mitosis, led us to a triple-color imaging strategy as depicted in Figure 2e. Specifically, our aim was to measure protein copy numbers as well as cluster distances of POIs in the kinetochore to build a molecular kinetochore map (TASK 1). Aside from labeling each POI, we thus needed a reference to identify cells in meta- to anaphase A as well as the orientation of the mitotic spindle and a centromeric reference serving as a landmark for kinetochore assembly in relation to the POIs. Therefore, we planned a triple-color strain library in which each strain contained the same two labeled reference proteins and a varying POI: As the reference proteins should have sufficient abundance, a defined organization and be present throughout the cell cycle, this led us to choose sad1, a protein from the spindle pole body (SPB) and the centromere-specific histone protein cnp1 (TASK 2) as references. From our imaging priority (TASK 3) and a mix of literature knowledge, a priori experience and several test strains and experiments we could deduce several measurement strategies solely relying on FPs (TASK 4), excluding blue and green fluorophores, some self-aggregating FPs as well as labeling strategies based on extrinsic labels or showing decreased S/N ratio or cross-talk problems (TASK 5). In our final, experimental study (manuscript in preparation) we use mScarlet-I [71], a bright red FP for the SPB reference and the UV-photoactivatable FP PAmCherry [72] as centromeric reference. Our highest priority on quantitative read-out of the POIs led us to choose the primed photoconvertible FP mEos3.2-A69T as POI-label [18,28].

several partners, highly efficient and specific labeling becomes a key factor. For example, two interaction partners, both labeled with a realistic efficiency of 50% would yield at best—when forming a permanent, static complex—only maximal 25% of positive co-localization (here we think of co-localization in an SMLM-specific definition of molecules being co-localized within an 'interaction radius' that takes localization precision and post-processing errors, labeling linkage distances, protein sizes and position of label attachment into account [79,80]). This observed co-localization of molecular partners easily drops further, e.g. for dynamic on/off-binding interaction equilibria dependent on different molecular conformations or when being misled by unspecific staining artifacts or lowered by slow FP maturation times. Here, counteractive knowledge on how to accumulate or arrest target molecules in certain molecular states by environmental changes (e.g. pH, temperature and nutrition), specific drug treatments (e.g. antibiotics compromising transcription, replication and cell wall organization) or by protein mutation might help the experiment. Additionally, target density easily restricts label choices. A clustered target in dense substructures demands for a high spatial resolution and tighter control of fluorophore read-out. Clustered targets can also be more challenging to label due to steric hindrances or label-dependent artificial aggregation artifacts as compared with an evenly distributed target within the cytoplasm [21,78,81–83].

When imaging living microorganisms, the shortest possible and least disturbing read-out option is desirable to avoid an excess of phototoxicity effects or changes in observed biology, e.g., the sensitivity of the investigated organism for specific wavelengths should be tested. Fast dynamics (e.g. free cytosolic Brownian diffusion or fast active transport) need a high temporal sampling to be resolved and to avoid confinement effects of the small microbial volumes. Contrarily, POIs slowed down by interactions with other cellular components (e.g. nucleoid-associated proteins or larger protein complexes) or by the viscosity of a certain compartment (e.g. in the membrane) allow for higher spatial resolution by the improved S/N of fluorescence read-out of slower acquisitions. Thus, it remains challenging but important to identify suitable sampling rates and read-out densities to correctly separate overlapping trajectories, to avoid confinement effects and to ensure being faster in read-out than biological alterations.

Transferring all mentioned requirements that can interfere with each other as best as possible into a practical experimental plan (Figure 5a, TASK 3) is the crucial key for a successful single-molecule sensitive microscopic

Table 3 Important factors to consider for a successful SMLM experiment Part 1 of 3

Labeling considerations	
Type of fluorophore	- **Control wild-type strain for specific autofluorescence in different spectral read-out channels** - **Evaluate the illumination intensities for different wavelengths for your specific organism. Which wavelengths and doses are tolerated, what are signs of phototoxicity? Generally, fluorophores of long wavelength and with low level of ROS production are favorable** - ***Evaluate your targets applicable orthogonal multi-targeting methods which go alongside with some fluorophore choices, e.g. FP utility depends on biologically undisturbed genetic fusions, dyes are extrinsic labels which are often not membrane-permeable and thus often need fixation protocols, etc.*** Signal detection at longer wavelengths typically improves S/N ratio, lowers phototoxicity and increases maximal imaging depth - ***Check for fluorophore-pair photophysics, e.g. brightness, bleaching rate, reversible blinking rates, preferably in the environment of your organism; check dye pairs for compatible switching buffers*** - Check FPs for compatible maturation times (e.g. faster than POI replenishment) and possible oligomerization tendencies (commonly dependent on POI abundance and density)
Functionality controls	- Control for biological function and localization of POIs by growth and functionality assays, western blot, tagging of POI by different fluorophore tags, C- or N-terminal or in-loop tagging variants, etc. - **Minor growth and functionality deficiencies might be compensated for by slower growth at lower temperatures**
Sample preparation	
Growth	- Use transparent, defined, sterile filtered medium to avoid background. If possible, avoid fluorescent supplements in medium - **Harvest cells in exponential growth phase, not in stationary phase** - **The optimal temperature for growth is not necessarily the optimal temperature for imaging, growth at lower temperatures might lead to less background in cells (but needs additional assays controlling for altered functionality)**
Ectopic induction of POI	- **Prepare fresh inducer stock from powder to avoid degradation effects ensuring reproducible induction conditions** - **Use only minimal concentrations of inducer (typically only a fraction of amounts from standard protocols) as overexpression of POI might cause high background fluorescence, inclusion bodies, aggregates or phenotype artifacts** - **After induction, allow for sufficient FP maturation time before imaging**
Fixation	- Optimal fixation conditions are target-, fluorophore- and organism-dependent. In general, fixation with 1–4% formaldehyde (final concentration) for 15–30 min is a good start. Addition of 0.05%–1% glutaraldehyde (final concentration) can improve the fixation results. Alternatively, also ice-cold methanol fixation can be tested - To quench excess formaldehyde, the first washing step with PBS should contain sodium borohydride or ammonium chloride - Several washing steps are needed to remove all excess formaldehyde - Carefully check if the fluorescence of the label or the spatial organization of your target is impaired by fixation
Staining	- Charge and size of dyes can lead to unspecific or insufficient staining - Blocking with neutral or charge masking compounds and/or intense washing with buffers containing higher salt concentrations (>100 mM) and low concentrations of detergent might reduce unspecific staining - Cell membrane permeabilization and **cell wall digestion improves staining** - **Prolonged staining combined with low (up to 1000-fold lower than conventional immunofluorescence) covalent dye/label concentrations can improve S/N ratio** - Use only minimal dye concentrations for live cell staining by electroporation/membrane-permeable dyes to avoid remaining free dyes - Perform a control staining of a sample without the target epitope to evaluate the degree of non-specific staining
Post-fixation	- For non-covalent labels with fixable groups, a finalizing post-fixation step following staining and washing prevents detachment of labels over time, which can be caused by the addition of thiol-containing imaging buffers
Cover glass slides	- Use high-precision cover glasses with defined thickness and matching the specifications of your objective - Clean thoroughly, prepare fresh - **For agarose pads, use high purity grade low gelling agarose to minimize heat degradation effects of the media which causes background and growth impairments**

Continued

Biochemical Society Transactions (2019) **47** 1041–1065
https://doi.org/10.1042/BST20180399

Table 3 Important factors to consider for a successful SMLM experiment Part 2 of 3

	- **For multi-well cover glasses, immobilize sample firmly onto a cover glass surface using poly-L-lysine (or organism-specific substances, e.g. ConA for targeting the α-linked mannose residues of the *S. cerevisiae* polysaccharides)**
General buffers	- Use high-quality chemicals with high purity grade for minimizing contaminants causing background - Prepare fresh and sterile filtered buffers - Use buffer with high salt concentration to wash out unwanted fluorescence (e.g. fluorescent metabolites, free fluorophores)
Fiducial markers	- Sonicate thoroughly prior to loading onto the sample to avoid fiducial aggregates - Adjust concentration to a density of at least three fiducials in focus in a typical ROI - Match fiducial brightness with sample brightness to prevent superposing the single-molecule signals during imaging - ***For imaging in two parallel channels: calibration slide (e.g. a fine spatial grid) of multi-colored fiducials for channel overlay***
Storage	- Check if sample quality (sample appearance, S/N and photoswitching efficiencies) is preserved after (long-term) storage at 4°C - Addition of sodium azide to fixed samples prevents the growth of contaminants
Imaging conditions	
Laser power	- Control laser power post-objective before each experiment - Adjust laser power (e.g. activation illuminations) for constant fluorophore blinking at sufficiently low density - Check for fluorophore bleaching
Illumination mode	- Laser power and background in the target plane change with applied imaging mode (epifluorescence, light sheet, HILO, TIRF) - Pulsing of the photoactivating lasers can reduce possible phototoxicity and offers temporal control for fluorophore activation
Switching buffers	- Quality demands as for general buffers above - ***Switching buffers have to be adjusted to both dyes of the selected dye combination*** - pH or redox components influence fluorophore switching behavior - Apply oxygen removing buffers directly before imaging and tightly seal the sample to prevent uptake of new atmospheric oxygen - Replace buffer regularly as enzymatic buffer exhaust themselves over time and might cause pH changes (e.g. GLOX buffer drops pH)
Imaging conditions and parameters	- Use appropriate immersion oil for your objective and avoid air bubbles in the oil - If implemented, use a focus-stabilizing system to avoid *z*-drift - ***Image fluorophores with excitation maxima at longer wavelengths first to avoid photobleaching and cross-talk*** - Camera frame rate should be fast enough to temporally resolve the molecule of interest kinetics - For structural studies, single fluorophore blinks should be recorded in only a few camera frames for maximal S/N - For 3D read-out: match the spatial resolution needed to answer your biological question with a compatible 3D technique. Read-out range and sensitivity is different for each 3D method
Imaging controls	- Negative: to check autofluorescence/background in all spectral channels used, a wild-type strain, a without correct epitope stained sample, for drug studies check non-treated strains - Positive: easy-to-image "standard strain" to control for stable setup configuration and thus constant read-out quality (S/N, photoswitching efficiencies) and to check for proper sample preparations. - Check for phototoxicity effects in live cell studies - **When imaging dynamics: prepare controls for (i) the freely diffusive cytosolic fluorophore(s) used as labels to benchmark the purely diffusive signal distribution (e.g. for confinement effects of small microbial volumes, possible inclusion bodies for overexpression) and (ii) a fixed control to access the immobile signal distribution (where the apparent movement is only determined by the acquired localization precision)**

Continued

Biochemical Society Transactions (2019) **47** 1041–1065
https://doi.org/10.1042/BST20180399

Table 3 Important factors to consider for a successful SMLM experiment Part 3 of 3

Post-processing prior data analysis	
Localization routine	- Check if the chosen localization algorithm fits fluorescent spots reliably - Determine the experimentally achieved localization precision - Check for fluorophore recall rates and false positives
Drift correction	- Use fiducial markers to correct for *x*–*y*-drift (by bead traces or cross-correlation) or apply cross-correlation on the target directly if possible (needs high fluorophore densities per frame, typically only possible for large ROIs and samples with highly abundant target molecule)
Channel alignment	- ***Parallel read-out: use a dense, ideally fine spatial grid as calibration sample for channel alignment before your experiment*** - ***For sequential read-out in the same spectral channel, fiducial markers are sufficient to overlay the image sequences***
Visualization	- Choose a visualization reflecting your achieved resolution to avoid interpretation errors (in co-localization, clustering analysis, etc.) - Choose a visualization with well-adjusted intensity scaling to mimic real fluorescence images one is used to
Data analysis	
Counting	- Characterize and quantify for over- and undercounting bias/error in your measurements
Clustering	- Optimize clustering algorithm thresholds/parameters to identify clusters properly while at the same time avoiding merging clusters into one cluster and omitting sparse molecules - Check and correct for self-clustering artifacts of blinking probes
Co-localization	- ***For live cell samples measured for long observation times (e.g. in sequential imaging modes or for long parallel read-out), control for possible target movements during the read-out time***
Dynamics	- Consider filtering trajectories for sufficient length (e.g. >6 steps) to provide enough statistics to extract robust diffusion characteristics

The table gives an overview of common tips and tricks and discusses the pitfalls of an SMLM experiment sorted by the different stages from study design over sample preparation to data analysis. Factors explicitly relevant for microbial samples are marked in bold; factors relevant for multi-color imaging in italics and bold.

study displaying its full potential. Thus, the more *a priori* knowledge of the measures needed to answer a specific biological question and of the characteristics of the target and its environment we have, the more straightforward is the selection of an appropriate combination of single-molecule targeting and read-out methods as discussed in the next paragraph (and in Figure 5a, lower box).

Selecting a suitable multi-color imaging strategy

When imaging multiple targets by multi-color SMLM one first has to choose groups of targets being imaged in parallel so that the signal of two sorts of fluorophores is detected at the same time, and/or sequential imaging, where the different targets are measured independently from each other and fluorescent signals are detected in a successive manner. For structural studies conducted in fixed samples which can be regarded as 'frozen biology' snapshots of immobile targets, this choice is only dependent on the selected fluorophore and labeling combination. Here, sequential imaging allows for subsequent addition of fluorophores which reduces channel cross-talk and prevents preterm photobleaching of only later read-out fluorophores. Furthermore, chromatic aberration can be circumvented by 'reusing' the same color channel [14,26–28]. Parallel imaging, on the other hand, reduces imaging times and allows for parallel drift correction. Chromatic aberrations can also be avoided by spectral demixing [53,55]. Next to the extremes of sequential and parallel imaging modes also an alternating read-out mode by orthogonal activation schemes can be applied, either using one [41] or several color channels [31,79].

When imaging living samples, parallel imaging is the primary choice for highly dynamic samples but technically highly limited. Here, dual-color sptPALM of interaction partners in microbes has been achieved by

Biochemical Society Transactions (2019) **47** 1041–1065
https://doi.org/10.1042/BST20180399

BiFC [36]. When using sequential imaging, at least one target should be considered temporally invariant [13,14,28,32,39,54], forced to be immobile by fast fixation [26,29,31], or both targets have to be regarded to be in dynamic equilibria states for the time of the experiment [28].

Criteria for suitable fluorophore combinations

Next to the biological constraints, technical factors restrict the repertoire of available fluorophore combinations that can be reliably used in multi-color SMLM (Figure 5a, lower box). Transferring the ideal list of desired fluorophore and labeling properties to the, in reality, still rather limited number of existing multi-color combinations of well-performing strategies usually only leaves a few choices—if any at all—and often requires simplification of the original experimental plans (returning to the first phase of study design as depicted in the upper box of Figure 5a).

Generally, as already introduced in Figure 4a, a fluorescent marker can be brought into the biological system by genetic fusions or by staining using immunolabeling, specific drugs, analogons or oligonucleotides dependent on the type of molecule of interest (protein, lipid, nucleic acid, etc.). Genetic fusions provide specific labeling in a one-to-one ratio which allows to visualize low abundant POIs or to quantify protein numbers (correcting for under- and overcounting effects [84]), whereas staining bears the risk of insufficient or unspecific labeling (e.g. due to dye charges, probe sizes or hydrophobicity). Only a few fluorescent dyes suited for SMLM studies are cell membrane-permeable, such as TMR, ATTO655 or the JF dye family [29,30,35,38,39]. Consequently, introducing dyes at high staining efficiencies into the crowded microbial organisms is challenging and dye delivery, as well as residual dye removal, needs to be assisted by membrane permeabilization or electroporation and cell wall digestion. Genetic fusions should be checked for growth and functionality deficiencies as some FPs tend to oligomerize [21,78,81–83] or might sterically hinder the protein function(s), e.g. shown for MreB in *E. coli* [74–76]. Finally, fluorescent dyes are commonly brighter and more photostable than FPs, improving read-out, but require specific switching buffers for photoblinking, which can be tricky to apply to live samples or can be toxic (e.g. depleting oxygen or adding strong reductants [2,6]). Here, different dyes might require different switching buffers which prevent their combined use. Also, FPs are influenced by switching buffers, e.g. oxygen removal prevents folding and reductants induce increased blinking [85,86]. Clever pairings of fluorophores and molecules of interest can compromise some drawbacks, e.g. when labeling and imaging a low abundance POI tagged with an FP first and only then staining the structural reference with a dye or when imaging the most dynamic POI by the brightest fluorophore of a chosen combination.

Nevertheless, taken all these limitations and requirements, it is not surprising that only a few fluorophore combinations perform well and lead to a full biological study after successfully passing TASK 4 and 5 in Figure 5a. These working combinations appear repeatedly in our literature review and often are specifically tailored. For example, dye staining is preferred for outer cell staining such as the cell wall, or brightness is often traded for probe specificity when using an FP tag for otherwise difficult-to-label POIs. In this respect, Tables 1 and 2 give a good overview of current working strategies and at the same time highlight the need for further probe developments.

Perspectives

Applying multi-color single-molecule imaging and tracking strategies remains challenging but yields essential results for our understanding of biological processes

The direct visualization and *in situ* measurement of the inner life of cells is essential for our understanding of biological processes and has led to many profound discoveries in biological research. Nevertheless, adapting and applying multi-color single-molecule imaging and tracking techniques in the various research fields remains challenging to this day. Behind each of the current microbial studies with their remarkable results hide individually tailored and often complex experimental designs. All the used single-molecule tools work close to current technology limits, and each new technological development allows for method improvement.

Recent (and future) probe developments might shift current technology limits

Current advances with promising results are for example brighter, fluorogenic or photoactivatable/photoswitchable probes [87–90], implementations of dye labels for single-molecule tracking with prolonged and more precise trajectories of different targets in microorganisms than traditionally obtained using FP labels in sptPALM imaging [91,92] or smaller (genetic) labels not interfering with cellular biology and/or allowing for high labeling densities and efficiencies [21,93].

How to best follow dynamic, co-moving interaction partners using SMLM methods remains an open question

To this day, there are no efficient tools for observing the dynamics of molecular interactions at a single-molecule resolution. One reason for this is the stochastic photoswitching read-out of probes. To follow both partners, both fluorophores have to emit light simultaneously. Currently, read-out of molecular interactions was realized by designing split versions of photochromic FPs for BiFC-PALM [36,94–96] or by energy transfer pairs using a photochromic donor [97], which, except for [36], were all conducted in mammalian cells. Both techniques, however, suffer from several drawbacks: Problems in BiFC-PALM stem from the irreversibility of FP complementation interfering with the imaged biology and the slow maturation of the complemented FP chromophores, which both prevent the dynamic study of transient short-lived interactions. Additionally, split-FPs have unneglectable tendencies of self-assembly, generating false-positive read-out signals. Photochromic fluorescence resonance energy transfer (FRET) approaches as reported in [97], however, suffer from almost halved fluorescence intensity read-outs drastically decreasing single-molecule resolution, direct acceptor excitation and acceptor bleaching and depend on extrinsic staining by far-red organic dyes as acceptors. Finally, all current photochromic approaches use UV-mediated photoconversion schemes which can interfere with cellular biology [18,98]. Thus, a protein interaction detection method inheriting the abilities of these tools, but being able to (i) reversibly monitor interaction dynamics (ii) at fast time scales, (iii) for prolonged imaging times and (iv) overcoming the current imaging artifacts will have a major impact when studying various fields of biology.

Abbreviations

AF, Alexa Fluor; BiFC, bimolecular fluorescence complementation; DaStPuRe, dark state pumping and recovery, illumination with high laser power forces the fluorophores into a dark state; dSTORM, direct stochastic optical reconstruction microscopy; EdU, 5-ethynyl-2′-deoxyuridine; FP, fluorescent protein; FRET, fluorescence resonance energy transfer; FROS, fluorescent repressor–operator system; HILO, highly inclined and laminated optical sheet; JF, Janelia Fluor; PAINT, point accumulation for imaging in nanoscale topography; PALM, photoactivated localization microscopy; PC-PALM, PALM using primed photoconversion; POIs, protein of interests; ROI, region of interest; S/N, signal-to-noise ratio; smFISH, single-molecule fluorescent *in situ* hybridization; SMLM, single-molecule localization microscopy; SPT, single-particle tracking; sptPALM, single-particle tracking PALM; TIRF, total internal reflection fluorescence; UV-PALM, PALM using UV-light photoactivation/conversion.

Author Contribution

I.V., J.W. and U.E. performed the literature review and created the tabular overviews, I.V. and J.W. conceived the figures, I.V. and U.E. wrote the manuscript with the help of J.W.

Funding

The authors gratefully acknowledge the Max Planck Society, SYNMIKRO and the Fonds der Chemischen Industrie for financial support.

Acknowledgements

We sincerely hope that we did not overlook any multi-color SMLM study conducted in microorganisms and would like to apologize to the authors if we did not include them in this summary. We furthermore thank David

Biochemical Society Transactions (2019) **47** 1041–1065
https://doi.org/10.1042/BST20180399

Virant, Bartosz Turkowyd and Alexander Balinovic for discussions and critical reading of the manuscript. Finally, we would like to thank all authors that provided us with figure data from their original publications to compile the overview figures 2 and 3.

Competing Interests

The authors declare that there are no competing interests associated with the manuscript.

References

1 Liu, Z., Lavis, L.D. and Betzig, E. (2015) Imaging live-cell dynamics and structure at the single-molecule level. *Mol. Cell* **58**, 644–659 https://doi.org/10.1016/j.molcel.2015.02.033
2 Turkowyd, B., Virant, D. and Endesfelder, U. (2016) From single molecules to life: microscopy at the nanoscale. *Anal. Bioanal. Chem.* **408**, 6885–6911 https://doi.org/10.1007/s00216-016-9781-8
3 Sigal, Y.M., Zhou, R. and Zhuang, X. (2018) Visualizing and discovering cellular structures with super-resolution microscopy. *Science* **361**, 880–887 https://doi.org/10.1126/science.aau1044
4 van de Linde, S., Löschberger, A., Klein, T., Heidbreder, M., Wolter, S., Heilemann, M. et al. (2011) Direct stochastic optical reconstruction microscopy with standard fluorescent probes. *Nat. Protoc.* **6**, 991–1009 https://doi.org/10.1038/nprot.2011.336
5 Adam, V., Berardozzi, R., Byrdin, M. and Bourgeois, D. (2014) Phototransformable fluorescent proteins: future challenges. *Curr. Opin. Chem. Biol.* **20**, 92–102 https://doi.org/10.1016/j.cbpa.2014.05.016
6 Endesfelder, U. (2016) Photoswitching fluorophores in super-Resolution fluorescence microscopy. *Super Resolution Imaging Biomed.* p. 49, CRC Press
7 Sahl, S.J. and Moerner, W.E. (2013) Super-resolution fluorescence imaging with single molecules. *Curr. Opin. Struct. Biol.* **23**, 778–787 https://doi.org/10.1016/j.sbi.2013.07.010
8 Xiao, J. and Dufrêne, Y.F. (2016) Optical and force nanoscopy in microbiology. *Nat. Microbiol.* **1**, 16186 https://doi.org/10.1038/nmicrobiol.2016.186
9 Kapanidis, A.N., Lepore, A. and El Karoui, M. (2018) Rediscovering bacteria through single-Molecule imaging in living cells. *Biophys. J.* **115**, 190–202 https://doi.org/10.1016/j.bpj.2018.03.028
10 Sharonov, A. and Hochstrasser, R.M. (2006) Wide-field subdiffraction imaging by accumulated binding of diffusing probes. *Proc. Natl Acad. Sci. U.S.A.* **103**, 18911–18916 https://doi.org/10.1073/pnas.0609643104
11 Heilemann, M., van de Linde, S., Schüttpelz, M., Kasper, R., Seefeldt, B., Mukherjee, A. et al. (2008) Subdiffraction-resolution fluorescence imaging with conventional fluorescent probes. *Angew. Chem. Int. Ed. Engl.* **47**, 6172–6176 https://doi.org/10.1002/anie.200802376
12 Bayas, C.A., Wang, J., Lee, M.K., Schrader, J.M., Shapiro, L. and Moerner, W.E. (2018) Spatial organization and dynamics of RNase E and ribosomes in *Caulobacter crescentus*. *Proc. Natl Acad. Sci. U.S.A.* **115**, E3712–E3721 https://doi.org/10.1073/pnas.1721648115
13 Bianchi, F., Syga, Ł., Moiset, G., Spakman, D., Schavemaker, P.E., Punter, C.M. et al. (2018) Steric exclusion and protein conformation determine the localization of plasma membrane transporters. *Nat. Commun.* **9**, 501 https://doi.org/10.1038/s41467-018-02864-2
14 Gahlmann, A., Ptacin, J.L., Grover, G., Quirin, S., von Diezmann, A.R.S., Lee, M.K. et al. (2013) Quantitative multicolor subdiffraction imaging of bacterial protein ultrastructures in three dimensions. *Nano Lett.* **13**, 987–993 https://doi.org/10.1021/nl304071h
15 McDonald, N.A., Lind, A.L., Smith, S.E., Li, R. and Gould, K.L. (2017) Nanoscale architecture of the *Schizosaccharomyces pombe* contractile ring. *eLife* **6**, 28865 https://doi.org/10.7554/eLife.28865
16 Ptacin, J.L., Lee, S.F., Garner, E.C., Toro, E., Eckart, M., Comolli, L.R. et al. (2010) A spindle-like apparatus guides bacterial chromosome segregation. *Nat. Cell Biol.* **12**, 791–798 https://doi.org/10.1038/ncb2083
17 Betzig, E., Patterson, G.H., Sougrat, R., Lindwasser, O.W., Olenych, S., Bonifacino, J.S. et al. (2006) Imaging intracellular fluorescent proteins at nanometer resolution. *Science* **313**, 1642–1645 https://doi.org/10.1126/science.1127344
18 Turkowyd, B., Balinovic, A., Virant, D., Carnero, H.G.G., Caldana, F., Endesfelder, M. et al. (2017) A general mechanism of photoconversion of green-to-red fluorescent proteins based on blue and infrared light reduces phototoxicity in live-cell single-molecule imaging. *Angew. Chem. Int. Ed. Engl.* **56**, 11634–11639 https://doi.org/10.1002/anie.201702870
19 Mohr, M.A., Kobitski, A.Y., Sabater, L.R., Nienhaus, K., Obara, C.J., Lippincott-Schwartz, J. et al. (2017) Rational engineering of photoconvertible fluorescent proteins for dual-color fluorescence nanoscopy enabled by a triplet-state mechanism of primed conversion. *Angew. Chem. Int. Ed. Engl.* **56**, 11628–11633 https://doi.org/10.1002/anie.201706121
20 Lampe, A., Haucke, V., Sigrist, S.J., Heilemann, M. and Schmoranzer, J. (2012) Multi-colour direct STORM with red emitting carbocyanines. *Biol. Cell* **104**, 229–237 https://doi.org/10.1111/boc.201100011
21 Virant, D., Traenkle, B., Maier, J., Kaiser, P.D., Bodenhöfer, M., Schmees, C. et al. (2018) A peptide tag-specific nanobody enables high-quality labeling for dSTORM imaging. *Nat. Commun.* **9**, 930 https://doi.org/10.1038/s41467-018-03191-2
22 Dempsey, G.T., Vaughan, J.C., Chen, K.H., Bates, M. and Zhuang, X. (2011) Evaluation of fluorophores for optimal performance in localization-based super-resolution imaging. *Nat. Methods* **8**, 1027–1036 https://doi.org/10.1038/nmeth.1768
23 Löschberger, A., van de Linde, S., Dabauvalle, M.-C., Rieger, B., Heilemann, M., Krohne, G. et al. (2012) Super-resolution imaging visualizes the eightfold symmetry of gp210 proteins around the nuclear pore complex and resolves the central channel with nanometer resolution. *J. Cell Sci.* **125**, 570–575 https://doi.org/10.1242/jcs.098822
24 Szymborska, A., de Marco, A., Daigle, N., Cordes, V.C., Briggs, J.A.G. and Ellenberg, J. (2013) Nuclear pore scaffold structure analyzed by super-resolution microscopy and particle averaging. *Science* **341**, 655–658 https://doi.org/10.1126/science.1240672
25 Durisic, N., Laparra-Cuervo, L., Sandoval-Álvarez, Á., Borbely, J.S. and Lakadamyali, M. (2014) Single-molecule evaluation of fluorescent protein photoactivation efficiency using an in vivo nanotemplate. *Nat. Methods* **11**, 156–162 https://doi.org/10.1038/nmeth.2784
26 Spahn, C., Cella-Zannacchi, F., Endesfelder, U. and Heilemann, M. (2015) Correlative super-resolution imaging of RNA polymerase distribution and dynamics, bacterial membrane and chromosomal structure in *Escherichia coli*. *Methods Appl. Fluoresc.* **3**, 014005 https://doi.org/10.1088/2050-6120/3/1/014005

27 Foo, Y.H., Spahn, C., Zhang, H., Heilemann, M. and Kenney, L.J. (2015) Single cell super-resolution imaging of *E. coli* ompR during environmental stress. *Integr. Biol.* **7**, 1297–1308 https://doi.org/10.1039/c5ib00077g
28 Virant, D. Turkowyd, B., Balinovic, A. and Endesfelder, U. (2017) Combining primed photoconversion and UV-photoactivation for aberration-free, live-cell compliant multi-color single-molecule localization microscopy imaging. *Int. J. Mol. Sci.* **18**, E1524 https://doi.org/10.3390/ijms18071524
29 Spahn, C.K., Glaesmann, M., Grimm, J.B., Ayala, A.X., Lavis, L.D. and Heilemann, M. (2018) A toolbox for multiplexed super-resolution imaging of the *E. coli* nucleoid and membrane using novel PAINT labels. *Sci. Rep.* **8**, 14768 https://doi.org/10.1038/s41598-018-33052-3
30 Karunatilaka, K.S., Cameron, E.A., Martens, E.C., Koropatkin, N.M., Biteen, J.S. and Ruby, E.G. (2014) Superresolution imaging captures carbohydrate utilization dynamics in human gut symbionts. *mBio* **5**, e02172 https://doi.org/10.1128/mBio.02172-14
31 Ptacin, J.L., Gahlmann, A., Bowman, G.R., Perez, A.M., von Diezmann, A.R.S., Eckart, M.R. et al. (2014) Bacterial scaffold directs pole-specific centromere segregation. *Proc. Natl Acad. Sci. U.S.A.* **111**, E2046–E2055 https://doi.org/10.1073/pnas.1405188111
32 Lew, M.D., Lee, S.F., Ptacin, J.L., Lee, M.K., Twieg, R.J., Shapiro, L. et al. (2011) Three-dimensional superresolution colocalization of intracellular protein superstructures and the cell surface in live *Caulobacter crescentus*. *Proc. Natl. Acad. Sci. U.S.A.* **108**, E1102–E1110 https://doi.org/10.1073/pnas.1114444108
33 Buss, J., Coltharp, C., Shtengel, G., Yang, X., Hess, H., Xiao, J. et al. (2015) A multi-layered protein network stabilizes the *Escherichia coli* FtsZ-ring and modulates constriction dynamics. *PLoS Genet.* **11**, e1005128 https://doi.org/10.1371/journal.pgen.1005128
34 Fei, J., Singh, D., Zhang, Q., Park, S., Balasubramanian, D., Golding, I. et al. (2015) RNA biochemistry. Determination of in vivo target search kinetics of regulatory noncoding RNA. *Science* **347**, 1371–1374 https://doi.org/10.1126/science.1258849
35 Fabiani, F.D., Renault, T.T., Peters, B., Dietsche, T., Gálvez, E.J.C., Guse, A. et al. (2017) A flagellum-specific chaperone facilitates assembly of the core type III export apparatus of the bacterial flagellum. *PLoS Biol.* **15**, e2002267 https://doi.org/10.1371/journal.pbio.2002267
36 Liu, Z., Xing, D., Su, Q.P., Zhu, Y. Zhang, J., Kong, X. et al. (2014) Super-resolution imaging and tracking of protein-protein interactions in sub-diffraction cellular space. *Nat. Commun.* **5**, 4443 https://doi.org/10.1038/ncomms5443
37 Vedyaykin, A.D., Gorbunov, V.V., Sabantsev, A.V., Polinovskaya, V.S., Vishnyakov, I.E. Melnikov, A.S. et al. (2015) Multi-color localization microscopy of fixed cells as a promising tool to study organization of bacterial cytoskeleton. *J. Phys. Conf. Series* **643**, 012020 https://doi.org/10.1088/1742-6596/643/1/012020
38 Wille, T., Barlag, B., Jakovljevic, V., Hensel, M., Sourjik, V., Gerlach, R.G. et al. (2015) A gateway-based system for fast evaluation of protein-protein interactions in bacteria. *PLoS ONE* **10**, e0123646 https://doi.org/10.1371/journal.pone.0123646
39 Barlag, B., Beutel, O., Janning, D., Czarniak, F., Richter, C.P., Kommnick, C. et al. (2016) Single molecule super-resolution imaging of proteins in living *Salmonella enterica* using self-labelling enzymes. *Sci. Rep.* **6**, 31601 https://doi.org/10.1038/srep31601
40 Zhang, Y., Lara-Tejero, M., Bewersdorf, J. and Galán, J.E. (2017) Visualization and characterization of individual type III protein secretion machines in live bacteria. *Proc. Natl Acad. Sci. U.S.A.* **114**, 6098–6103 https://doi.org/10.1073/pnas.1705823114
41 Berk, V., Fong, J.C.N., Dempsey, G.T., Develioglu, O.N., Zhuang, X., Liphardt, J. et al. (2012) Molecular architecture and assembly principles of *Vibrio cholerae* biofilms. *Science* **337**, 236–239 https://doi.org/10.1126/science.1222981
42 Fiche, J.B., Cattoni, D.I., Diekmann, N., Langerak, J.M., Clerte, C., Royer, C.A. et al. (2013) Recruitment, assembly, and molecular architecture of the SpoIIIE DNA pump revealed by superresolution microscopy. *PLoS Biol.* **11**, e1001557 https://doi.org/10.1371/journal.pbio.1001557
43 Liao, Y., Schroeder, J.W., Gao, B., Simmons, L.A. and Biteen, J.S. (2015) Single-molecule motions and interactions in live cells reveal target search dynamics in mismatch repair. *Proc. Natl Acad. Sci. U.S.A.* **112**, E6898–E6906 https://doi.org/10.1073/pnas.1507386112
44 Fleming, T.C., Shin, J.Y., Lee, S.H., Becker, E., Huang, K.C., Bustamante, C. et al. (2010) Dynamic SpoIIIE assembly mediates septal membrane fission during *Bacillus subtilis* sporulation. *Genes. Dev.* **24**, 1160–1172 https://doi.org/10.1101/gad.1925210
45 Yen Shin, J., Lopez-Garrido, J., Lee, S.H., Diaz-Celis, C., Fleming, T., Bustamante, C. et al. (2015) Visualization and functional dissection of coaxial paired SpoIIIE channels across the sporulation septum. *eLife* **4**, e06474 https://doi.org/10.7554/eLife.06474
46 Wang, W., Li, G.-W., Chen, C., Xie, X.S. and Zhuang, X. (2011) Chromosome organization by a nucleoid-associated protein in live bacteria. *Science* **333**, 1445–1449 https://doi.org/10.1126/science.1204697
47 Stracy, M., Jaciuk, M., Uphoff, S., Kapanidis, A.N., Nowotny, M., Sherratt, D.J. et al. (2016) Single-molecule imaging of UvrA and UvrB recruitment to DNA lesions in living *Escherichia coli*. *Nat. Commun.* **7**, 12568 https://doi.org/10.1038/ncomms12568
48 Stracy, M., Lesterlin, C., Garza de Leon, F., Uphoff, S., Zawadzki, P. and Kapanidis, A.N. (2015) Live-cell superresolution microscopy reveals the organization of RNA polymerase in the bacterial nucleoid. *Proc. Natl Acad. Sci. U.S.A.* **112**, E4390–E4399 https://doi.org/10.1073/pnas.1507592112
49 Garza de Leon, F., Sellars, L., Stracy, M., Busby, S.J.W. and Kapanidis, A.N. (2017) Tracking low-copy transcription factors in living bacteria: the case of the lac repressor. *Biophys. J.* **112**, 1316–1327 https://doi.org/10.1016/j.bpj.2017.02.028
50 Vedyaykin, A.D., Vishnyakov, I.E. Polinovskaya, V.S., Khodorkovskii, M.A. and Sabantsev, A.V. (2016) New insights into FtsZ rearrangements during the cell division of *Escherichia coli* from single-molecule localization microscopy of fixed cells. *Microbiologyopen* **5**, 378–386 https://doi.org/10.1002/mbo3.336
51 Vedyaykin, A.D., Sabantsev, A.V., Vishnyakov, I.E. Morozova, N.E. and Khodorkovskii, M.A. (2017) Recovery of division process in bacterial cells after induction of SulA protein which is responsible for cytokinesis arrest during SOS-response. *Cell Tissue Biol.* **11**, 89–94 https://doi.org/10.1134/S1990519X17020080
52 Robinson, A., McDonald, J.P., Caldas, V.E.A., Patel, M., Wood, E.A., Punter, C.M. et al. (2015) Regulation of mutagenic DNA polymerase V activation in space and time. *PLoS Genet.* **11**, e1005482 https://doi.org/10.1371/journal.pgen.1005482
53 Ries, J., Kaplan, C., Platonova, E., Eghlidi, H. and Ewers, H. (2012) A simple, versatile method for GFP-based super-resolution microscopy via nanobodies. *Nat. Methods* **9**, 582–584 https://doi.org/10.1038/nmeth.1991
54 Hajj, B., Wisniewski, J., El Beheiry, M., Chen, J., Revyakin, A., Wu, C. et al. (2014) Whole-cell, multicolor superresolution imaging using volumetric multifocus microscopy. *Proc. Natl Acad. Sci. U.S.A.* **111**, 17480–17485 https://doi.org/10.1073/pnas.1412396111
55 Zhao, T., Wang, Y., Zhai, Y., Qu, X., Cheng, A., Du, S. et al. (2015) A user-friendly two-color super-resolution localization microscope. *Opt. Express* **23**, 1879–1887 https://doi.org/10.1364/OE.23.001879
56 Mund, M., van der Beek, J.A., Deschamps, J., Dmitrieff, S., Hoess, P., Monster, J.L. et al. (2018) Systematic nanoscale analysis of endocytosis links efficient vesicle formation to patterned actin nucleation. *Cell* **174**, 884–896.e17 https://doi.org/10.1016/j.cell.2018.06.032

57 Puchner, E.M., Walter, J.M., Kasper, R., Huang, B. and Lim, W.A. (2013) Counting molecules in single organelles with superresolution microscopy allows tracking of the endosome maturation trajectory. *Proc. Natl Acad. Sci. U.S.A.* **110**, 16015–16020 https://doi.org/10.1073/pnas.1309676110
58 Zhou, L., Obhof, T., Schneider, K., Feldbrügge, M., Nienhaus, G.U. and Kämper, J. (2018) Cytoplasmic transport machinery of the SPF27 homologue Num1 in *Ustilago maydis*. *Sci. Rep.* **8**, 3611 https://doi.org/10.1038/s41598-018-21628-y
59 Ishitsuka, Y., Savage, N., Li, Y., Bergs, A., Grün, N., Kohler, D. et al. (2015) Superresolution microscopy reveals a dynamic picture of cell polarity maintenance during directional growth. *Sci. Adv.* **1**, e1500947 https://doi.org/10.1126/sciadv.1500947
60 Virant, D., Vojnovic, I., Winkelmeier, J., Rigl, M. and Endesfelder, U. Investigation of the kinetochore structure of *Schizosaccharomyces pombe* by quantitative single-molecule localization microscopy imaging. Manuscript in preparation
61 Sustarsic, M., Plochowietz, A., Aigrain, L., Yuzenkova, Y., Zenkin, N. and Kapanidis, A. (2014) Optimized delivery of fluorescently labeled proteins in live bacteria using electroporation. *Histochem. Cell Biol.* **142**, 113–124 https://doi.org/10.1007/s00418-014-1213-2
62 Di Paolo, D., Afanzar, O., Armitage, J.P. and Berry, R.M. (2016) Single-molecule imaging of electroporated dye-labelled CheY in live *Escherichia coli*. *Philos. Trans. R. Soc. Lond. B Biol. Sci.* **371**, 20150492 https://doi.org/10.1098/rstb.2015.0492
63 Saurabh, S., Perez, A.M., Comerci, C.J., Shapiro, L. and Moerner, W.E. (2016) Super-resolution imaging of live bacteria cells using a genetically directed, highly photostable fluoromodule. *J. Am. Chem. Soc.* **138**, 10398–10401 https://doi.org/10.1021/jacs.6b05943
64 Raulf, A., Spahn, C.K., Zessin, P.J.M., Finan, K., Bernhardt, S., Heckel, A. et al. (2014) Click chemistry facilitates direct labelling and super-resolution imaging of nucleic acids and proteins. *RSC Adv.* **4**, 30462–30466 https://doi.org/10.1039/C4RA01027B
65 Kipper, K., Lundius, E.G. Ćurić, V., Nikić, I., Wiessler, M., Lemke, E.A. et al. (2017) Application of noncanonical amino acids for protein labeling in a genomically recoded *Escherichia coli*. *ACS Synth. Biol.* **6**, 233–255 https://doi.org/10.1021/acssynbio.6b00138
66 Liang, H., DeMeester, K.E., Hou, C.-W., Parent, M.A., Caplan, J.L. and Grimes, C.L. (2017) Metabolic labelling of the carbohydrate core in bacterial peptidoglycan and its applications. *Nat. Commun.* **8**, 15015 https://doi.org/10.1038/ncomms15015
67 Crawford, R., Torella, J.P., Aigrain, L., Plochowietz, A., Gryte, K., Uphoff, S. et al. (2013) Long-lived intracellular single-molecule fluorescence using electroporated molecules. *Biophys. J.* **105**, 2439–2450 https://doi.org/10.1016/j.bpj.2013.09.057
68 Volkov, I.L., Lindén, M., Aguirre Rivera, J., Ieong, K.-W., Metelev, M., Elf, J. et al. (2018) tRNA tracking for direct measurements of protein synthesis kinetics in live cells. *Nat. Chem. Biol.* **14**, 618–626 https://doi.org/10.1038/s41589-018-0063-y
69 Muyrers, J.P., Zhang, Y. and Stewart, A.F. (2001) Techniques: recombinogenic engineering – new options for cloning and manipulating DNA. *Trends Biochem. Sci.* **26**, 325–331 https://doi.org/10.1016/S0968-0004(00)01757-6
70 Bremer, H. and Dennis, P.P. (1996) Modulation of chemical composition and other parameters of the cell by growth rate. In *Escherichia coli and Salmonella*, 2nd edn (Neidhardt, F.C., ed.), pp. 1553–1569, ASM Press, Washington, DC
71 Bindels, D.S., Haarbosch, L., van Weeren, L., Postma, M., Wiese, K.E., Mastop, M. et al. (2017) mScarlet: a bright monomeric red fluorescent protein for cellular imaging. *Nat. Methods* **14**, 53–56 https://doi.org/10.1038/nmeth.4074
72 Subach, F.V., Patterson, G.H., Manley, S., Gillette, J.M., Lippincott-Schwartz, J. and Verkhusha, V.V. (2009) Photoactivatable mCherry for high-resolution two-color fluorescence microscopy. *Nat. Methods* **6**, 153–626 https://doi.org/10.1038/nmeth.1298
73 Narsing Rao, M.P., Xiao, M. and Li, W.J. (2017) Fungal and bacterial pigments: secondary metabolites with wide applications. *Front. Microbiol.* **8**, 1113 https://doi.org/10.3389/fmicb.2017.01113
74 Bendezu, F.O., Hale, C.A., Bernhardt, T.G and de Boer, P.A.J. (2009) RodZ (YfgA) is required for proper assembly of the MreB actin cytoskeleton and cell shape in *E. coli*. *EMBO J.* **28**, 193–204 https://doi.org/10.1038/emboj.2008.264
75 Swulius, M.T. and Jensen, G.J. (2012) The helical MreB cytoskeleton in *Escherichia coli* MC1000/pLE7 is an artifact of the N-terminal yellow fluorescent protein tag. *J. Bacteriol.* **194**, 6382–6386 https://doi.org/10.1128/JB.00505-12
76 Lee, T.K., Tropini, C., Hsin, J., Desmarais, S.M., Ursell, T.S., Gong, E. et al. (2014) A dynamically assembled cell wall synthesis machinery buffers cell growth. *Proc. Natl Acad. Sci. U.S.A.* **111**, 4554–4559 https://doi.org/10.1073/pnas.1313826111
77 Wu, B., Piatkevich, K.D., Lionnet, T., Singer, R.H and Verkhusha, V.V. (2011) Modern fluorescent proteins and imaging technologies to study gene expression, nuclear localization, and dynamics. *Curr. Opin. Cell Biol.* **23**, 310–317 https://doi.org/10.1016/j.ceb.2010.12.004
78 Wang, S., Moffitt, J.R., Dempsey, G.T., Xie, X.S. and Zhuang, X. (2014) Characterization and development of photoactivatable fluorescent proteins for single-molecule-based superresolution imaging. *Proc. Natl Acad. Sci. U.S.A.* **111**, 8452–8457 https://doi.org/10.1073/pnas.1406593111
79 Malkusch, S., Endesfelder, U., Mondry, J., Gelléri, M., Verveer, P.J. and Heilemann, M. (2012) Coordinate-based colocalization analysis of single-molecule localization microscopy data. *Histochem. Cell Biol.* **137**, 1–10 https://doi.org/10.1007/s00418-011-0880-5
80 Aaron, J.S., Taylor, A.B. and Chew, T.L. (2018) Image co-localization – co-occurrence versus correlation. *J. Cell Sci.* **131**, jcs211847 https://doi.org/10.1242/jcs.211847
81 Landgraf, D., Okumus, B., Chien, P., Baker, T.A and Paulsson, J. (2012) Segregation of molecules at cell division reveals native protein localization. *Nat. Methods* **9**, 480–482 https://doi.org/10.1038/nmeth.1955
82 Zhang, M., Chang, H., Zhang, Y., Yu, J., Wu, L., Ji, W. et al. (2012) Rational design of true monomeric and bright photoactivatable fluorescent proteins. *Nat. Methods* **9**, 727–729 https://doi.org/10.1038/nmeth.2021
83 Stockmar, I., Feddersen, H., Cramer, K., Gruber, S., Jung, K., Bramkamp, M. et al. (2018) Optimization of sample preparation and green color imaging using the mNeonGreen fluorescent protein in bacterial cells for photoactivated localization microscopy. *Sci. Rep.* **8**, 10137 https://doi.org/10.1038/s41598-018-28472-0
84 Jung, S.R., Fujimoto, B.S. and Chiu, D.T. (2017) Quantitative microscopy based on single-molecule fluorescence. *Curr. Opin. Chem. Biol.* **39**, 64–73 https://doi.org/10.1016/j.cbpa.2017.06.004
85 Subach, F.V., Malashkevich, V.N., Zencheck, W.D., Xiao, H., Filonov, G.S., Almo, S.C. et al. (2009) Photoactivation mechanism of PAmCherry based on crystal structures of the protein in the dark and fluorescent states. *Proc. Natl Acad. Sci. U.S.A.* **106**, 21097–21102 https://doi.org/10.1073/pnas.0909204106
86 Endesfelder, U., Malkusch, S., Flottmann, B., Mondry, J., Liguzinski, P., Verveer, P.J. et al. (2011) Chemically induced photoswitching of fluorescent probes – a general concept for super-resolution microscopy. *Molecules* **16**, 3106–3118 https://doi.org/10.3390/molecules16043106
87 Grimm, J.B., English, B.P., Choi, H., Muthusamy, A.K., Mehl, B.P., Dong, P. et al. (2016) Bright photoactivatable fluorophores for single-molecule imaging. *Nat. Methods* **13**, 985–988 https://doi.org/10.1038/nmeth.4034

88 Ke, N., Landgraf, D., Paulsson, J. and Berkmen, M. (2016) Visualization of periplasmic and cytoplasmic proteins with a self-labeling protein tag. *J. Bacteriol.* **198**, 1035–1043 https://doi.org/10.1128/JB.00864-15
89 Lavis, L.D. (2017) Teaching old dyes new tricks: biological probes built from fluoresceins and rhodamines. *Annu. Rev. Biochem.* **86**, 825–843 https://doi.org/10.1146/annurev-biochem-061516-044839
90 Gautier, A. and Tebo, A.G. (2018) Fluorogenic protein-based strategies for detection, actuation, and sensing. *Bioessays* **40**, e1800118 https://doi.org/10.1002/bies.201800118
91 Yu, A. (2017) *Towards Resolving the Yeast Replisome In Vivo*, McGill University Libraries, Mc Gill University
92 Banaz, N., Mäkelä, J. and Uphoff, S. (2018) Choosing the right label for single-molecule tracking in live bacteria: Side-by-side comparison of photoactivatable fluorescent protein and halo tag dyes. *J. Phys. D Appl. Phys.* **52**, 064002 https://doi.org/10.1088/1361-6463/aaf255
93 Strauss, S., Nickels, P.C., Strauss, M.T., Jimenez Sabinina, V., Ellenberg, J., Carter, J.D. et al. (2018) Modified aptamers enable quantitative sub-10-nm cellular DNA-PAINT imaging. *Nat. Methods* **15**, 685–688 https://doi.org/10.1038/s41592-018-0105-0
94 Xia, P., Liu, X., Wu, B., Zhang, S., Song, X., Yao, P.Y. et al. (2014) Superresolution imaging reveals structural features of EB1 in microtubule plus-end tracking. *Mol. Biol. Cell* **25**, 4166–4173 https://doi.org/10.1091/mbc.e14-06-1133
95 Nickerson, A., Huang, T., Lin, L.-J. and Nan, X. (2015) Photoactivated localization microscopy with bimolecular fluorescence complementation (BiFC-PALM). *J. Vis. Exp.* **106**, e53154 https://doi.org/10.3791/53154
96 Chen, M., Liu, S., Li, W., Zhang, Z., Zhang, X., Zhang, X.-E. et al. (2016) Three-fragment fluorescence complementation coupled with photoactivated localization microscopy for nanoscale imaging of ternary complexes. *ACS Nano* **10**, 8482–8490 https://doi.org/10.1021/acsnano.6b03543
97 Basu, S., Needham, L.-M., Lando, D., Taylor, E.J.R., Wohlfahrt, K.J., Shah, D. et al. (2018) FRET-enhanced photostability allows improved single-molecule tracking of proteins and protein complexes in live mammalian cells. *Nat. Commun.* **9**, 2520 https://doi.org/10.1038/s41467-018-04486-0
98 Wäldchen, S., Lehmann, J., Klein, T., van de Linde, S. and Sauer, M. (2015) Light-induced cell damage in live-cell super-resolution microscopy. *Sci. Rep.* **5**, 15348 https://doi.org/10.1038/srep15348